THE FLORIDA STATE UNIVERSITY

COLLEGE OF ARTS AND SCIENCES

PREDICTING WARM SEASON NOCTURNAL CLOUD-TO-GROUND LIGHTNING NEAR CAPE CANAVERAL, FLORIDA

By

CHRISTOPHER E. CANTRELL

A thesis submitted to the
Department of Meteorology
in partial fulfillment of the
Requirements for the degree of
Master of Science

Degree Awarded:

Summer Semester, 1999

REPORT DOCUMENTATION PAGE	Form Approved OMB No. 0704-0188

1. AGENCY USE ONLY *(Leave blank)*	2. REPORT DATE	3. REPORT TYPE AND DATES COVERED
	23.Aug.99	THESIS

4. TITLE AND SUBTITLE
PREDICTING WARM SEASON NOCTURNAL CLOUD-TO-GROUND LIGHTNING NEAR CAPE CANAVERAL. FLORIDA

5. FUNDING NUMBERS

6. AUTHOR(S)
CAPT CANTRELL CHRISTOPHER E

7. PERFORMING ORGANIZATION NAME(S) AND ADDRESS(ES)
FLORIDA STATE UNIVERSITY

8. PERFORMING ORGANIZATION REPORT NUMBER

9. SPONSORING/MONITORING AGENCY NAME(S) AND ADDRESS(ES)
THE DEPARTMENT OF THE AIR FORCE
AFIT/CIA, BLDG 125
2950 P STREET
WPAFB OH 45433

10. SPONSORING/MONITORING AGENCY REPORT NUMBER
FY99-254

11. SUPPLEMENTARY NOTES

12a. DISTRIBUTION AVAILABILITY STATEMENT
Unlimited distribution
In Accordance With AFI 35-205/AFIT Sup 1

12b. DISTRIBUTION CODE

13. ABSTRACT *(Maximum 200 words)*

14. SUBJECT TERMS	15. NUMBER OF PAGES
	71
	16. PRICE CODE

17. SECURITY CLASSIFICATION OF REPORT	18. SECURITY CLASSIFICATION OF THIS PAGE	19. SECURITY CLASSIFICATION OF ABSTRACT	20. LIMITATION OF ABSTRACT

The members of the Committee approve the thesis of Christopher E. Cantrell defended on July 6, 1999.

Henry E. Fuelberg

Henry E. Fuelberg
Professor Directing Thesis

T N Krishnamurti

T. N. Krishnamurti
Committee Member

Jon E. Ahlquist

Jon E. Ahlquist
Committee Member

ACKNOWLEDGEMENTS

This research was funded by the Air Force Weather Agency (AFWA) from sub-award S96-75662 to Florida State University from the Cooperative Program for Operational Meteorology, Education and Training (COMET) under a cooperative agreement between the National Oceanic and Atmospheric Administration (NOAA) and the University Corporation for Atmospheric Research (UCAR). The views herein are those of the author, and do not necessarily reflect the views of NOAA, its sub-agencies, or UCAR.

I would like to acknowledge Global Atmospherics, Inc. in Tucson, Arizona for providing the NLDN cloud-to-ground lightning flash data.

I deeply appreciate the time and effort Dr. Henry Fuelberg, my major professor, has given to the shaping, refining, and compilation of this research. His attention to detail and extensive knowledge of meteorology are responsible for making this thesis a clear, concise, and complete work. Thank you Dr. Fuelberg. I would like to thank Dr. Jon Ahlquist and Dr. T.N. Krishnamurti for their guidance during my research.

The personnel at the 45th Weather Squadron also provided much support and insight. Special thanks go to Mr. Bill Roeder. I would also like to thank Mrs. Susan Derussy of Computer Sciences Raytheon for providing data necessary for this research.

I would be remiss if I did not thank my friends in the lab. First, I thank Jon Kelly,

Joe Maloney, and Todd Lericos for their help in getting me started and familiarizing me with the computer programs I used in this research. I would also like to thank Rick Lusher, John Hannan, Jeff Cupo, Anil Rao, and Matt Duke for their time and support.

Most importantly, I wish to thank my wife, Uyen, and daughter, Emma. Their love, patience, understanding, and support through it all mean more than they will ever know.

TABLE OF CONTENTS

LIST OF TABLES

LIST OF FIGURES

Figure Page

ABSTRACT

Two aspects of nocturnal convection over Florida are examined in this study: A climatology of all warm season nocturnal cloud-to-ground lightning (CGL) flashes over east central Florida, and nocturnal CGL that develops near Cape Canaveral, Florida during undisturbed conditions. Seven years of warm season (May – October) radiosonde data (1992 – 1998) are used to categorize nights into one of five wind regimes based on the 1000 – 700 mb mean vector wind. Cloud-to-ground flashes are used to examine the spatial distribution of nocturnal lightning. Flashes are found to occur on 525 of the 825 nights with available soundings. Spatial maps of CGL flashes reveal that most occur over the Gulf Stream.

Nights with flow parallel to the peninsula from the south are found to have the greatest percent occurrence of nights with CGL flashes. Enhanced midlevel moisture (700 – 500 mb) increases the percent occurrence of nights having CGL flashes. Midlevel lapse rates (850 – 500 mb) show little variation among the wind regimes. Streamline analyses reveal that the synoptic flow is crucial in determining thermodynamic characteristics of air over the study area.

Data from the local lightning detection network reveal 74 nights during the warm season months of 1995 – 1997 with cloud-to-ground lightning within a 40 km radius of study. Surface analyses are used to eliminate nights with disturbed flow, while radar data

are analyzed to eliminate pre-existing convection. A data set of nights without CGL (NCGL nights) also is constructed. Stability, temperature, wind, and moisture parameters of the two categories are examined statistically.

The 1000 – 800 mb lapse rate is the only temperature related parameter that statistically discriminates between the two categories. Relative humidities at 850, 800, and 750 mb all show statistically significant discrimination between categories. The K-Index is found to have the greatest forecast skill of all the standard stability parameters. A Modified K-Index created using the 1000 – 800 mb lapse rate and the 850 – 700 mb moisture provides the best statistical discrimination and forecast skill of all the wind and thermodynamic parameters examined.

1. INTRODUCTION

The state of Florida has the greatest frequency of thunderstorm days in the United States. These storms occur mostly during the summer months. Numerous studies have been conducted in the natural thunderstorm laboratory that exists over the state. These studies have focused on topics such as lightning climatology, the spatial and diurnal distribution of lightning and convection, and the use of synoptic regimes and thermodynamic parameters to forecast convection.

Orville (1991) produced the first map of cloud-to-ground (CGL) flash densities over the United States. Based on one year of data (1989), he identified central Florida as having the greatest concentration of flashes in the nation (10 flashes per square kilometer). Many researchers have studied the spatial and diurnal distribution of lightning and convection over Florida (e.g., Lopez et al. 1984; Blanchard and Lopez 1985; Watson et al. 1991; Maier and Krider 1984; Reap 1994; Watson and Holle 1996; Camp et al. 1998). These studies emphasized the role that diurnal heating, sea breezes, and coastline shape play on the distribution of lightning.

Research on convection over Florida also has focused on the correlation between convection and synoptic patterns. Many studies have documented the importance of the synoptic-scale wind flow on the distribution of convection over the Florida peninsula (e.g., Byers and Rodebush 1948; Gentry and Moore 1954; Estoque 1962; Frank et al.

1967; Neumann 1971a, b; Pielke 1974; Blanchard and Lopez 1985; Watson et al. 1987). For example, using 18-hour sea level pressure forecasts from the Nested Grid Model (NGM), Reap (1994) defined the lightning distribution associated with the seven flow patterns that occur most frequently over Florida during the warm season. In a study of spatial patterns of convection in South Florida, Blanchard and Lopez (1985) defined three map types based on rainfall patterns. Both studies emphasized the important role that synoptic-scale flow patterns play in the development of convection over Florida during the warm season.

Thermodynamic parameters and stability indices also have been studied in the forecasting of convection over Florida. Blanchard and Lopez (1985), Watson et al. (1991), Lopez et al. (1994), and Laird et al. (1995) showed the importance of mid-level moisture on the development and intensity of convection over Florida. Other studies have determined the stability indices that are useful for forecasting Florida convection (e.g., Neumann 1971; Reap 1994; Bauman 1995; Fuelberg and Biggar 1996; Kelly 1998).

All of the aforementioned studies have emphasized convection during either the 24-hour day or during the daytime only. To the author's knowledge, no study has documented the nocturnal thunderstorm climatology for east central Florida, or has quantified the conditions that are most favorable for nocturnal CGL. Also, no study has documented nocturnal thunderstorm development during undisturbed surface synoptic patterns over the Kennedy Space Center (KSC). This void in existing knowledge presents an excellent opportunity to investigate nocturnal convection.

This study investigates nocturnal thunderstorms over east central Florida. Two aspects are considered. First, a climatology of warm season nocturnal CGL flashes over

east central Florida is presented. Nights with flashes are categorized into five low-level wind regimes. The temporal and spatial distributions of CGL flashes, as well as the thermodynamic parameters associated with each regime, are documented during a seven-year period. Second, warm season nocturnal thunderstorms that develop near the Kennedy Space Center and Cape Canaveral, Florida are investigated. Thermodynamic parameters and stability indices are examined for possible use as a forecast tool for storm development near KSC during undisturbed synoptic patterns. This study hopes to provide forecasters at the United States Air Force 45th Weather Squadron (45WS) with information that will increase their understanding of nocturnal thunderstorms in their area of forecast responsibility.

2. DATA AND METHODOLOGY

a. Nocturnal CGL Climatology

The area of study for the nocturnal CGL climatology is defined by a rectangle approximately 2° latitude × 3° longitude (Fig. 1). Centered just east of the Kennedy Space Center (KSC) at 28.6°N, 80.4°W, the 57,400 km^2 area encompasses east central Florida. This region was chosen to include the KSC, the Orlando area to the west, Daytona Beach to the north, and Patrick Air Force Base to the south. The study area also extends off the east coast of Florida to include the western portion of the Gulf Stream. The period of the CGL flash climatology comprises the warm season months of May through October of 1992 through 1998.

The three main data sources for the nocturnal CGL climatology were CGL flashes detected by the National Lightning Detection Network (NLDN), upper air soundings from Cape Canaveral Air Station (CCAS), and reanalysis data from the National Centers for Environmental Prediction (NCEP)/National Center for Atmospheric Research (NCAR). The availability of sounding data was established first. Specifically, available evening soundings were matched with nights containing CGL flashes. This created a data set of nights having both sounding data and lightning data.

Radiosondes normally are launched at the CCAS three times per day (1000, 1500, and 2200 UTC). However, these launch times can vary depending on operational needs.

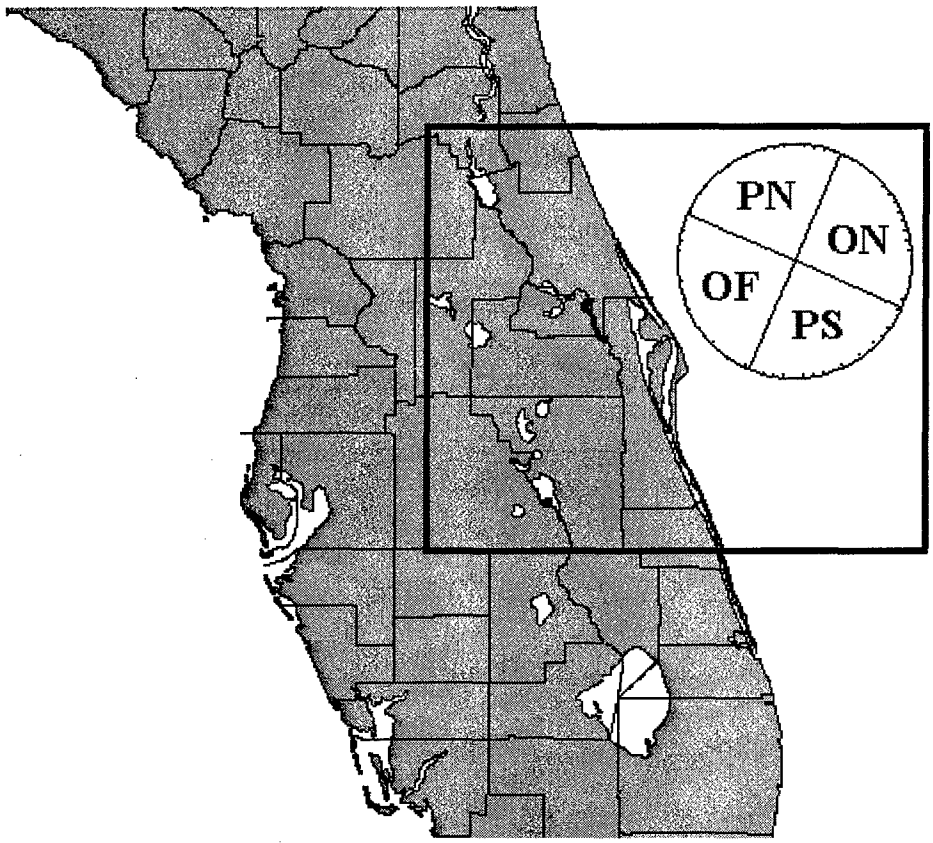

Fig. 1. Area for the climatology of nocturnal CGL flashes over east central Florida. Flow regimes are indicated in the inset and are based on the direction from which the 1000 – 700 mb mean vector wind is blowing, i.e., parallel north (PN), onshore (ON), parallel south (PS), and offshore (OF).

To include as many days as possible in the climatology, we used one evening sounding per day taken between 2100 to 0000 UTC. The sounding data were provided by the National Climatic Data Center. Of the 1288 days comprising the warm seasons of 1992 through 1998, 825 soundings were available for analysis.

The 825 soundings next were categorized into one of five wind regimes based on the 1000 to 700 mb vector mean wind. This classification scheme was used by Lopez and Holle (1997) in a study of lightning over central Florida, and by Watson et al. (1991) in a study of CGL flashes over the KSC. Specifically, two perpendicular and two parallel 90 degree sectors were defined based on the northwest (338°) to southeast (158°) orientation of mainland east coast Florida (Fig. 1). The two perpendicular regimes are onshore (ON) flow (024° – 113°) and offshore (OF) flow (204° – 293°). The two parallel regimes are parallel flow from the north (PN) (294° – 023°) and parallel flow from the south (PS) (114° – 203°). The fifth regime, calm (CLM) flow, includes days with mean speeds less than 2 m s^{-1} regardless of wind direction. Once the wind regimes were established, the NLDN lightning data were examined to determine nights that contained CGL flashes.

Of the 825 evenings with soundings, 525 (64%) were found to have at least one CGL flash between 0200 to 1300 UTC. This 11-hour period defines nocturnal convection for this investigation. The beginning time of 0200 UTC was chosen instead of sunset in an attempt to eliminate lingering convection that had formed during the afternoon and early evening hours. Sunset times during the warm season months vary widely, from a maximum of 0024 UTC during July to a minimum of 2253 UTC during October (Fig. 2). The beginning time of 0200 UTC is at least one hour and thirty minutes

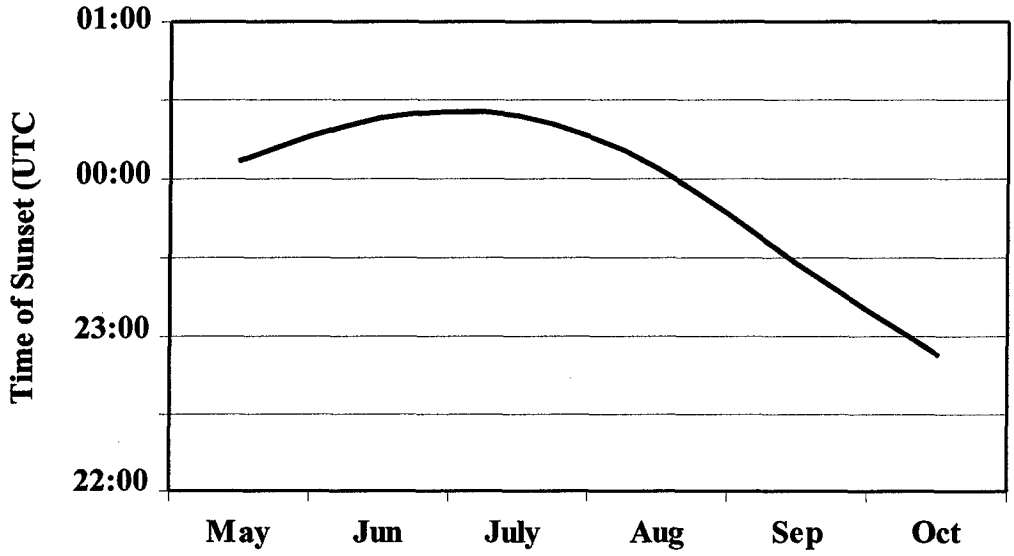

Fig. 2. Time of sunset at the Kennedy Space Center for the warm season months of May through October.

after sunset in all cases.

Global Atmospherics, Inc. in Tucson, Arizona provided the NLDN lightning data. The NLDN consists of 106 magnetic direction finders that record CGL flashes over the contiguous United States and adjacent coastal waters (Cummins et al. 1998). Time, location, polarity, intensity, and number of return strokes are recorded for each flash.

The NLDN does not detect every CGL flash; however, two upgrades to the NLDN during our period of study (1992 and 1995) have significantly increased its detection efficiency and location accuracy. For example, the detection efficiency of the network has increased from 65% - 80% (1989-1994) to 80% - 90% (1995 – Present). The location accuracy also has improved with each successive upgrade, going from 4 – 8 km (1989 – 1991) to 2 – 4 km (1992 – 1994) to 0.5 – 1.0 km (1995 – Present). Cummins et al. (1998) and Orville (1987, 1994) give a more detailed description of the detection methodology and sensors.

Spatial maps of CGL location were constructed using a 56 × 41 grid. This grid utilized 5 km × 5 km boxes to bin individual CGL flashes according to their latitude and longitude. The total number of flashes in each box was divided by 25 to give flashes per square kilometer, and then by the number of years in the study. This produced a display of average warm season nocturnal flash density per square kilometer. Total flashes in each wind regime, as well as hourly flash counts, also were examined.

The five wind regimes were examined using streamline analyses at 1000 and 700 mb. Lopez et al. (1984) and Blanchard and Lopez (1985) used similar streamline maps at these two levels in their studies of convection over South Florida. The analyses were constructed using daily averages of u- and v-wind components from NCEP/NCAR

reanalysis data provided by the NOAA-CIRES Climate Diagnostics Center, Boulder, Colorado, from their Web site at http://www.cdc.noaa.gov/. A detailed description of the NCEP/NCAR reanalysis project can be found in Kalnay et al. (1996).

b. Nocturnal Thunderstorms near Cape Canaveral, Florida

This portion of the research focused on warm season nocturnal convection that forms near Cape Canaveral, Florida during undisturbed synoptic flow. The region of interest is bounded by a circle of 40 km radius, with an area of 5027 km^2, that is centered just southwest of the NASA Shuttle Landing Facility (SLF) (Fig. 3). The 45th Weather Squadron (45WS) is responsible for providing lightning warnings and forecasts to the KSC and the CCAS. Our study region includes all of the 45WS lightning warning and forecast areas and is similar to that used by Kelly (1998). The period of study for this phase of research includes the warm season months of May through October of 1995 through 1997.

The data used in this component of the study were from the local lightning detection network operated by KSC, surface meteorological analyses, the Melbourne National Weather Service (NWS) Weather Surveillance Radar-88 Doppler (WSR-88D), and radiosonde soundings launched at 2215 UTC from the CCAS.

The KSC Cloud-to-Ground Lightning Surveillance System (CGLSS) provided the time and location of strikes within the study area (Harms et al. 1997). The CGLSS has a strike detection accuracy of 92 percent, an effective range of 100 km, and a location accuracy of 0.5 km. Using data from the CGLSS, 552 days from the warm seasons of 1995-1997 were examined for the occurrence of nocturnal CGL strikes.

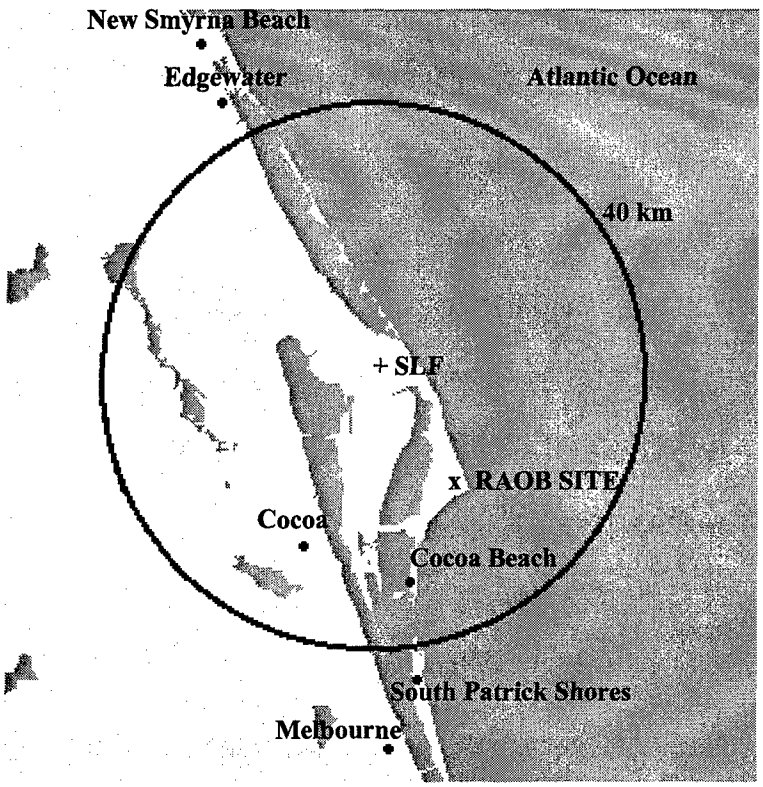

Fig. 3. Map of the Cape Canaveral area. Study area lies within the 40 km radius circle centered near the Shuttle Landing Facility (SLF).

Based on these lightning data, a set of nocturnal thunderstorm events was established. Specifically, the initial step was to identify nights having CGL flashes within the area of interest. The time period examined spanned 0200 UTC (2200 EDT) until 1300 UTC (0900 EDT). As stated earlier, the beginning time of 0200 UTC was chosen instead of sunset in the hope of eliminating lingering convection that had formed during the afternoon and early evening hours. One or more nocturnal CGL flashes was found within the 40 km radius on 74 of the 552 days (13.4 percent).

The 74 nocturnal CGL events were scrutinized to eliminate those that were associated with surface synoptic forcing mechanisms. NCEP surface analyses were utilized to eliminate disturbed days containing cold fronts, stationary fronts, troughs, tropical depressions, tropical storms and/or hurricanes. Inspection of the analyses eliminated all but the 38 cases of nocturnal convection that were associated with undisturbed flow.

Radar imagery from the Melbourne NWS WSR-88D was used to examine storm formation on the 38 undisturbed days. Convection was required to form after sunset and to produce its first CGL flash within the area of study. A day was eliminated if the convection did not meet these requirements. This final screening process produced the final set of 19 undisturbed CGL cases. Unfortunately, 7 of the 19 evening soundings were not available. Therefore, only 12 nights with CGL were available for sounding and stability parameter comparisons. Thermodynamic parameters and stability indices from the soundings of these 12 nights pertinent to statistical and forecasting skill calculations discussed in Chapter 4 are listed in Table A1 of the appendix.

A data set of nights having no CGL flashes in the study area (null cases) also was

selected. The objective was to determine which atmospheric parameters and stability indices best discriminate between CGL and non-CGL (NCGL) nights. We strived to select NCGL nights immediately preceding or following a CGL night. This would allow us to determine the atmospheric changes that occurred from one day to the next. This selection was not always possible due to some instances of consecutive nights with CGL. There also were NCGL nights that did not meet the undisturbed surface synoptic requirement or did not have an available evening sounding. The final null data set consisted of 32 cases, with 50 percent of them either preceding or following a CGL night. All 32 NCGL nights had an available evening sounding. Thermodynamic parameters and stability indices from the soundings of these 32 nights pertinent to statistical and forecasting skill calculations are listed in Table A2 of the appendix.

General Meteorological PAcKage (GEMPAK) routines from the National Centers Advanced Weather Interactive Processing System (N-AWIPS) were used to calculate seven stability parameters (K-Index, Lifted Index, Total Totals, Convective Available Potential Energy (CAPE), Convective Inhibition (CIN), Showalter Index, and the Level of Free Convection (LFC)) for each CGL and NCGL day. For the Lifted Index, the parcel being lifted was the layer 100 m above the surface. For CAPE and CIN the lifted parcel was the lowest 500 m of the atmosphere.

An examination of stability parameters and vertical profiles of temperature, relative humidity, and u- and v-wind components revealed differences between the CGL and NCGL days. We performed a significance test to determine which atmospheric parameters best distinguished between the two groups. The skewed nature of the data rendered the standard t-test inappropriate. However, Mielke et al. (1976, 1981) has

developed a non-parametric test for investigating univariate and multivariate distributions. This statistical test, called the multi-response permutation procedure (MRPP), avoids the t-test assumption that a data sample must follow a normal distribution. Blanchard and Lopez (1985) used MRPP to determine the statistical significance of atmospheric parameters between four recurring convective pattern types in South Florida. Kelly (1998) also successfully used MRPP in his study of the east coast sea breeze near Cape Canaveral, Florida.

MRPP computes the average difference between values of various groups. A simple weighted mean then is calculated to determine the separation between values of the groups. This weighted mean is compared to all possible weighted means that can be obtained for the two groups. The comparison yields the observed significance level (p-value). A p-value < 0.05 indicates that values are from different populations at the 95 % or higher confidence level. A detailed description of the procedure can be found in Mielke et al. (1981).

In assessing the statistical significance of differences in stability indices and atmospheric parameters between CGL and NCGL nights, the problem of serial correlation was considered. Specifically, day-to-day data often are not independent. Therefore, a subset of 12 CGL and 32 NCGL nights with soundings was chosen so there was at least a 6 day gap between chronologically ordered days in each category. The result of this screening left 10 CGL and 22 NCGL nights available for the MRPP calculations. This procedure was used only in calculating MRPP p-values.

Once the MRPP results had indicated the statistically significant parameters between the two categories, three methods were used to determine the ability of these

parameters to successfully forecast a CGL day verses a NCGL day: Critical Success Index (CSI), Heidke Skill Score (HSS), and the True Skill Statistic (TSS).

Donaldson et al. (1975) described the CSI method for evaluating the skill of severe weather predictions. Using a basic 2 × 2 contingency table (Table 1), three of the four elements are used to define the CSI as

$$\mathrm{CSI} \equiv x / (x + y + z). \tag{1}$$

This index has been used widely in operational forecast verification. CSI has a range of +1 to 0, where a score of +1 indicates a perfect forecast. A limitation of this procedure is that it does not consider correct forecasts of null events. Stated another way, the w-element of the contingency table is not considered. This limitation is amplified when forecasting rare events. The HSS and TSS do incorporate the w-element information from Table 1.

The Heidke Skill Score (Heidke 1926) is defined by Panofsky and Brier (1958) as

$$\begin{aligned} \mathrm{HSS} &= C - E / N - E \\ &= 2(xw - yz) / y^2 + z^2 + 2xw + (y + z)(x + w), \end{aligned} \tag{2}$$

where C is the number of correct forecasts $(x + w)$, N is the total number of forecasts $(x + y + z + w)$, and E is defined as

$$\mathrm{E} = (x + z)(x + y) + (z + w)(y + w) / x + y + z + w. \tag{3}$$

E is the expected number of correct forecasts due purely to chance. The HSS has a range from –1 to +1, with +1 indicating a perfect forecast.

Doswell and Flueck (1989) described the TSS method for evaluating the skill of forecasts during the DOPLIGFHT '87 field research project. Watson et al. (1991), Fuelberg and Biggar (1994), and Kelly (1998) successfully used TSS in studies of Florida

Table 1. Schematic forecast contingency table using the notation of Donaldson et al. (1975).

	Observed		
Forecast	**Yes**	**No**	**Total**
Yes	x	z	$x + z$
No	y	w	$y + w$
Total	$x + y$	$z + w$	N

convection. TSS is defined as

$$\text{TSS} = \text{POD} - \text{POFD} = (xw - yz) / (x + y)(z + w), \quad (4)$$

where POD is the Probability of Detection and POFD is the Probability of False Detection. TSS provides a measure of actual forecast performance compared to perfect performance. Like the HSS, the TSS also has a range of +1 to –1, where a score of +1indicates a perfect forecast, while a TSS of 0 indicates no skill.

An iterative process was employed to determine for each predictor the threshold value that produced the greatest TSS score. Each value within the sample of a predictor was allowed to be the threshold. A TSS then was calculated based on that threshold. This process was repeated for all values within the sample. The value that produced the greatest TSS score was chosen as the threshold value for that predictor. The TSS is the statistics that receives the most consideration in this study.

In order to confirm the optimum TSS scores using thresholds selected by the iterative scheme, a bootstrap method was used (Wilks 1995). The method is desirable due to the small data set being evaluated. One advantage of bootstrap is that it makes no assumptions about the original sample, i.e., the distribution is not required to be normal. Bootstrap builds numerous additional samples by replicating the original sample. Specifically, a random index, corresponding to one of the indices assigned to the original sample values, is generated to pick a value from the sample. This random selection is repeated until the new sample contains the same number of values as the original one. For the purpose of this study, 5000 samples, based on the original, were generated. The iterative process discussed previously is performed on these sets of new samples to produce a set of corresponding thresholds. A histogram is constructed of these sets of

thresholds that produced the greatest TSS score to determine which threshold has the greatest percent occurrence, and thus is the optimum threshold value for the predictor being considered.

3. NOCTURNAL CLOUD-TO-GROUND CLIMATOLOGY

One or more CGL flashes occurred between 0200 to 1300 UTC on 525 nights for which soundings were available during the warm season months of 1992 through 1998. This number represents 64 percent of the 825 evenings with available soundings. All synoptic situations (fronts, troughs, tropical depressions, and hurricanes) are included in this climatology. Therefore, the storm or system that produces the lightning flashes does not necessarily originate within the study area. In addition, some of the CGL flashes are not from convection that develops after sunset. That is, CGL flashes produced by convection forming before 0200 UTC and persisting into the time period are included.

a. Nocturnal CGL Distribution

Before categorizing nights with CGL into the five wind regimes, it is important to show the map of all CGL flashes occurring between 0200 to 1300 UTC (Fig. 4). Ten years of CGL data for the months May – October from 1989 to 1998 were available for constructing this map. CGL flashes were normalized by the number of years in the sample, yielding a spatial distribution of flashes per warm season. A total of 357,691 nocturnal flashes was recorded in the region during the period of study. The most striking feature is the number of flashes over water as compared to the amount over land. Flashes over water amount to 86 percent of the total number of CGL in the study area,

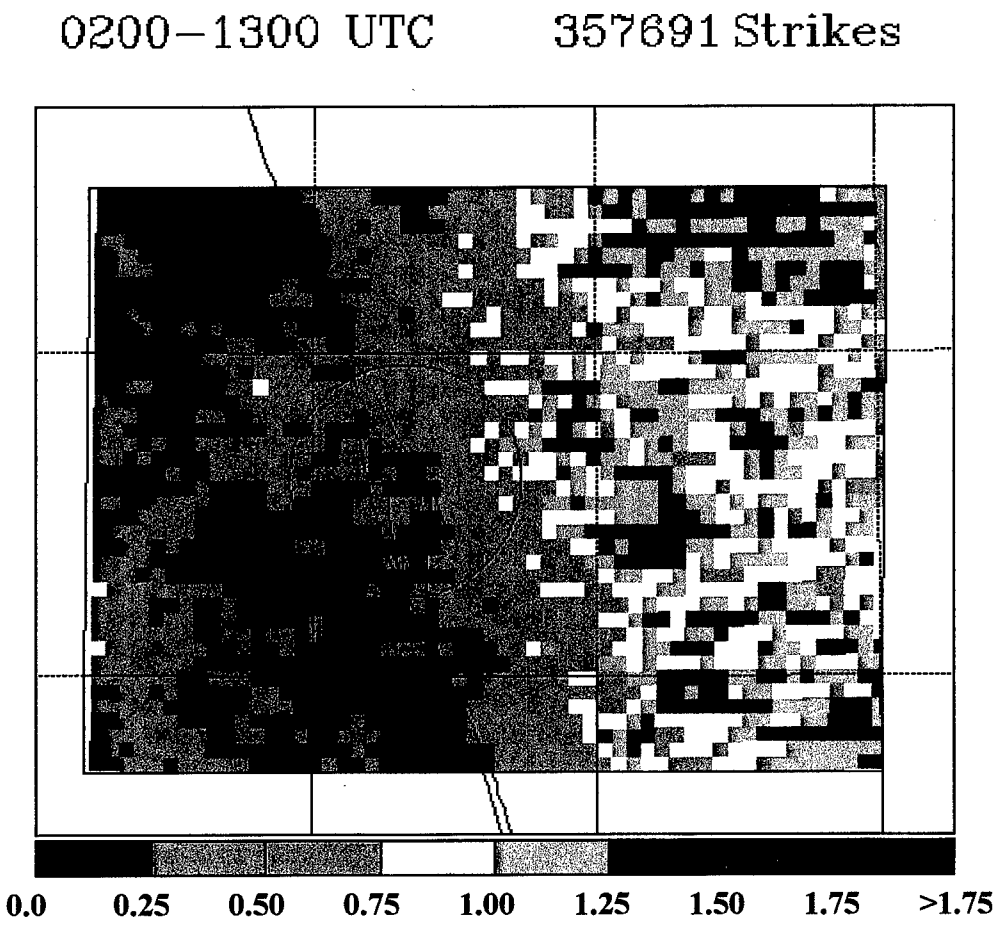

Fig. 4. Composite of average warm season nocturnal CGL flashes per square kilometer from May to October of 1989-1998.

while flashes over water total only 14 percent. Concentrations of densities greater than 0.75 flashes per square kilometer extend from approximately 40 km off the coast to the eastern edge of the study area. This area of enhanced flash densities suggests that nocturnal CGL is closely linked to the warm waters of the Gulf Stream. Flash densities onshore generally are less than 0.25 flashes per square kilometer.

The percent of nights having CGL flashes within the five low level flow regimes is shown in Fig. 5. The OF category has the most nights (244) and CGL nights (169), while the CLM category has the fewest nights (94) and CGL nights (63). Although the PS flow category ranks third in the number of nights (167) and second in the number of CGL nights (129), it exhibits the greatest percent of nights with CGL. That is, 77 percent of PS nights contain CGL. PN and ON exhibit the smallest percent of nights with CGL. Only 50 percent of PN nights and 52 percent of ON nights contain CGL.

Spatial maps of nocturnal CGL flash distribution for the five flow regimes provide insight into nighttime lightning (Fig. 6). These nocturnal CGL flash distributions are based on the warm season months of 1992 through 1998. Since sounding data for 1989 – 1991 were not available, the time period for these maps differs from that of the composite map (Fig. 4). Any nocturnal CGL flashes on nights without sounding data are not included in the maps.

The ON flow category has the smallest number of nocturnal flashes of any regime (11,470; Table 2), and the smallest median number of flashes per day (14). This is not surprising given the thermodynamic properties of the flow that are discussed in the following section. Unlike the other regimes, ON flow exhibits a minimum of percent flashes per hour at the beginning of the period (Fig. 7b). The percent of flashes per hour

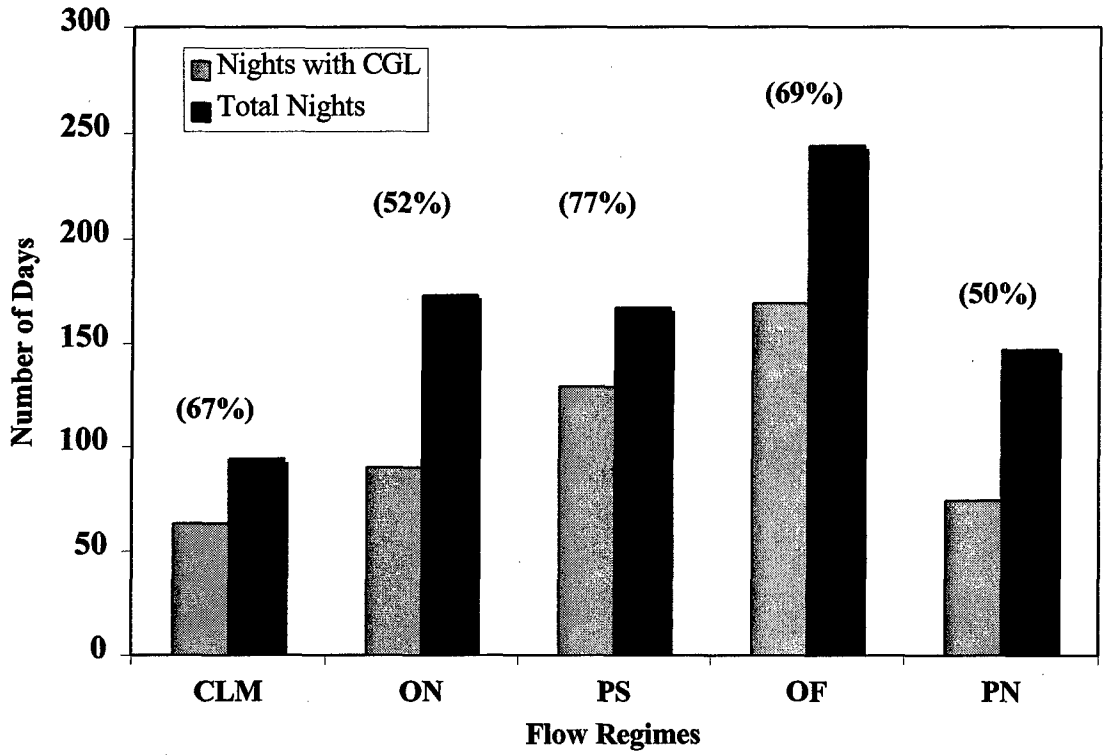

Fig. 5. Distribution of nights with CGL and total nights according to flow regime. Percent occurrence of nights with CGL to total nights for individual regimes is shown in parenthesis.

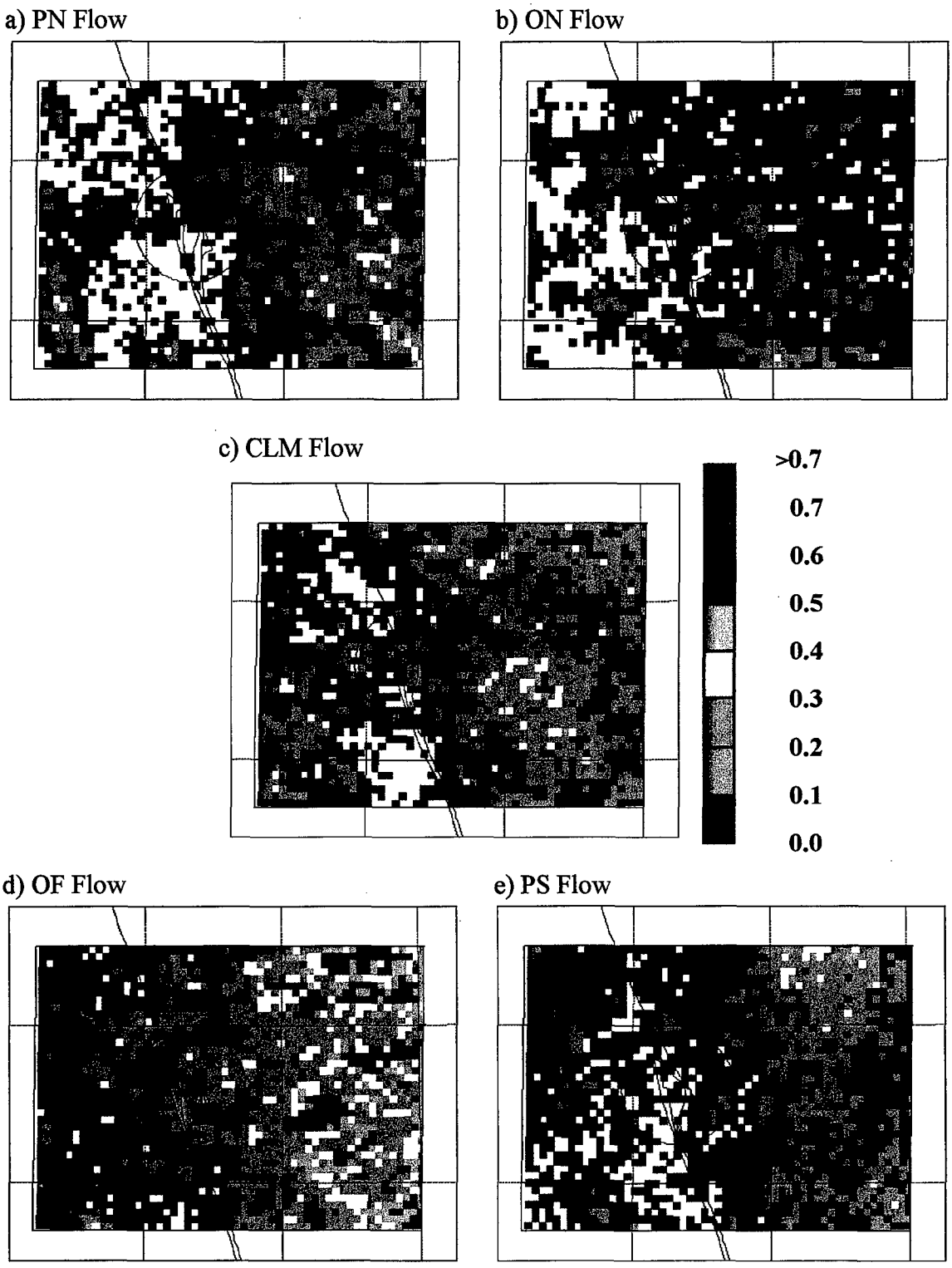

Fig. 6. Composite of warm season average nocturnal CGL flashes per square kilometer from May to October of 1992 – 1998 for a) PN flow, b) ON flow, c) CLM flow, d) OF flow, and e) PS flow. The label bar indicates number of flashes per square kilometer.

Table 2. CGL flash statistics for each flow regime. Rankings of the median number of flashes per day are given in parentheses.

Category	Total Flashes	Nights With CGL	Mean	Min	25th Percentile	Median	75th Percentile	Max	SD
ON	11470	90	127	1	3	14 (5)	115	2871	358
PN	26242	74	355	1	4	30 (4)	319	5251	852
CLM	35693	63	567	1	15	37 (3)	533	4582	1106
PS	24611	129	191	1	7	47 (2)	188	2065	344
OF	75636	169	448	1	8	103 (1)	472	4633	809

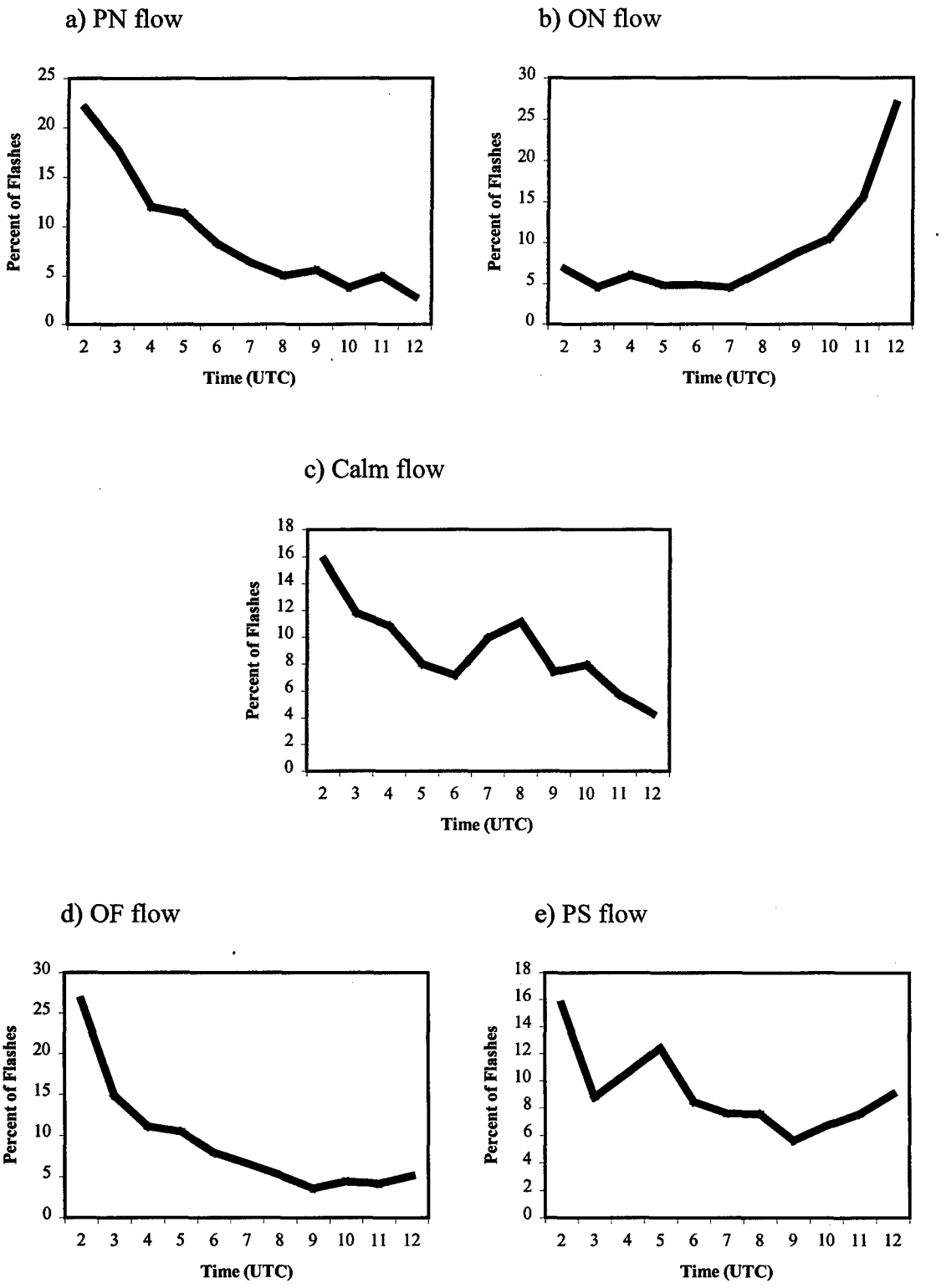

Fig. 7. Temporal distribution profiles for a) PN flow, b) ON flow, c) Calm flow, d) OF flow, and e) PS flow.

remains steady through the night until 0700 UTC when it begins increasing, reaching a maximum of 27 percent during the 1200 UTC hour.

Scattered areas of local maxima characterize the ON flow category distribution (Fig 6b). The pattern for the ON regime also is influenced by a small percent (6%) of the days (5) producing a majority percentage (54%) of the flashes (6,163).

Nights with PN flow rank third in flash amount, producing 26,242 nocturnal flashes over 74 days (Table 2), and rank fourth in median number of flashes per day (30). The temporal distribution of flashes (Fig. 7a) shows a maximum of 22 percent at 0200 UTC, gradually decreasing during the night and reaching a minimum of 3 percent at 1200 UTC.

The pattern of nocturnal CGL for PN flow (Fig. 6a) shows numerous areas of local maxima. The majority of these maxima are located over the Gulf Stream; however, one is over land to the southeast of KSC. This map, combined with the fact that 53 percent of the flashes (13,924) occur on only 5 percent of the CGL days (4), indicates that these maxima also are associated with individual storms. Note, however, that a majority of the flashes occur over the Gulf Stream.

The 63 CLM nights (< 2 m s^{-1}) produce 35,693 flashes during the period (Table 2). With a median flash count of 37, this category ranks third out of the five regimes. Figure 7c shows that the maximum percent of flashes occurs during the 0200 UTC hour. A secondary peak occurs during the 0800 UTC hour. The minimum percent of flashes occurs during the 1200 UTC hour.

The spatial distribution of flashes on CLM nights (Fig. 6c) shows an area of maximum densities over the Gulf Stream just east of KSC. Weaker maxima are located

west and southwest of KSC. With 54 percent of the flashes (19,165) occurring on only 8 percent of the CGL days (5), the spatial distribution is dominated by a few storms that produce a majority of the flashes.

Parallel flow from the south (PS) ranks second in the median number of flashes per day (47), but ranks fourth in number of flashes (24,611) during 129 flow days (Table 2). The primary maximum of flashes occurs at 0200 UTC, but there is a secondary maximum during the 0500 UTC hour (Fig. 7e). The spatial distribution map for PLS flow (Fig. 6e) again highlights the role of the Gulf Stream in producing CGL flashes. A north – south maximum is evident over the area of the Gulf Stream that is northeast of Cape Canaveral.

The final, and most active flow regime is OF. It ranks first in both the number of flashes (75,636) and the median number of flashes per day (103). CGL flashes are most numerous during the 0200 UTC hour, when 27 percent of them occur (Fig. 7d). The activity gradually diminishes, reaching a minimum of 4 percent during the 0900 UTC hour. The OF flash distribution (Fig. 6d) shows the greatest density of flashes over the Gulf Stream of all the regimes. Many areas exhibit densities of 0.5 flashes per square kilometer or greater.

b. Atmospheric and Synoptic Flow Characteristics

To gain a better understanding of differences between flash data of the five flow regimes, thermodynamic properties and streamline maps for each regime are presented next. Instability and moisture are important ingredients for the development of convection. Table 3 presents the percent occurrence of nights with CGL, along with the

700 – 500-mb mean relative humidity (RH), and 850 – 500-mb lapse rate. The ranking of each parameter in the wind regime categories of CGL nights and NCGL nights also is shown.

A commonly used parameter in thunderstorm prediction is the 850 – 500 mb lapse rate. Stability indices such as the K-Index and Total-Totals use this lapse rate in their calculations of thunderstorm probability.

Calm (CLM) CGL nights have the greatest lapse rate of all categories (5.81° C km^{-1}). The ON NCGL nights show the most stable conditions with the smallest lapse rate of all categories (5.35° C km^{-1}). The lapse rate for each CGL category is greater than its corresponding NCGL category, except the PS regime. However, the greatest difference in lapse rate between CGL and NCGL nights is only 0.26 C km^{-1} in the ON regime. The greatest difference among the CGL groups is only 0.20 C km^{-1} between the CLM and ON regime. Figure 8 shows mean soundings for CGL nights (solid lines) and NCGL nights (dashed lines) for the all days composite and the five different flow regimes. The temperature soundings reveal the small difference in lapse rate and temperature between CGL days and NCGL days.

These findings suggest that variations in the 850 – 500-mb lapse rate do not explain nocturnal lightning occurrence over east central Florida. For example, PS nights have the greatest percent occurrence of CGL but rank fourth in lapse rate strength (Table 3). OF shows the closest agreement between lapse rate (ranked second) and percent occurrence of CGL days (ranked second).

Adequate moisture is needed for convective development. The mean soundings (Fig. 8) show differences in midlevel moisture in each flow regime. CGL nights having

Table 3. Average moisture and stability characteristics for all flow regimes and the five individual CGL and NCGL wind regime categories. Rankings are in parentheses.

Flow Regime	Percent Occurrence (Rank)	700–500 mb RH (%)	850–500 mb Lapse rate (°C/km)
CGL Flash Nights			
PS	77 (1)	64 (1)	5.67 (4)
OF	69 (2)	60 (2)	5.73 (2)
CLM	67 (3)	55 (3)	5.81 (1)
ON	52 (4)	53 (4)	5.61 (5)
PN	50 (5)	50 (5)	5.72 (3)
ALL	64	58	5.70
NCGL Flash Nights			
PS	23 (5)	53 (1)	5.69 (1)
OF	31 (4)	41 (2)	5.65 (2)
CLM	33 (3)	39 (3)	5.60 (3)
ON	48 (2)	33 (5)	5.35 (5)
PN	50 (1)	34 (4)	5.57 (4)
ALL	36	38	5.53

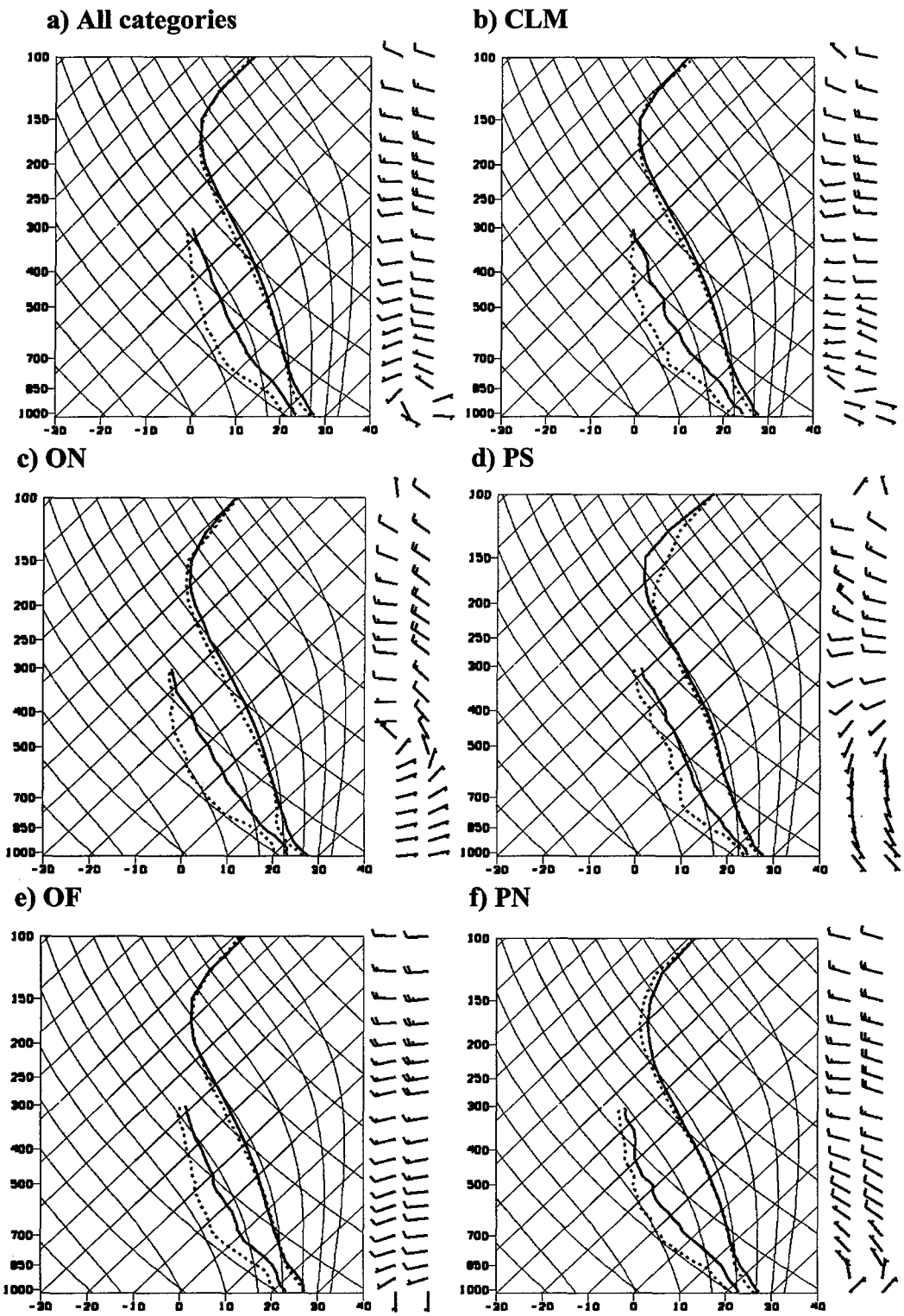

Fig. 8. Mean CCAS soundings for nights with CGL (solid) and NCGL (dashed) for a) all categories, b) CLM regime, c) ON regime, d) PS regime, e) OF regime, and f) PN regime. CGL winds are in the left column, with NCGL winds in the right column.

PS flow exhibit the greatest midlevel RH (64 percent), while NCGL nights having ON flow show the smallest midlevel RH (33 percent) (Table 3). Within the CGL category, PN flow exhibits the lowest relative humidity (50 percent), and also is least effective at producing nocturnal lightning. Rankings of midlevel relative humidity for the remaining three regimes of nights with CGL also correspond well with the percent occurrence of CGL nights. An examination of 1000 – 850-mb and 850 - 700-mb relative humidity (not shown) indicates little difference between CGL flow regimes. Results for total column precipitable water (not shown) are similar to those of 700 – 500-mb average relative humidity. Current findings agree with those of Burpee (1979), Lopez et al. (1984), and Watson et al. (1991), who noted that enhanced midlevel relative humidity is associated with a greater likelihood of lightning. In our case it appears that moisture, especially midlevel moisture, is a good indicator of nocturnal CGL.

Atmospheric moisture is partially controlled by the larger scale flow. To further understand moisture characteristics of the five wind regimes, streamline analyses for each are examined at 1000 and 700 mb (Fig. 9-13).

Streamlines at 1000 mb for the PS nights (Fig. 9a) indicate southeasterly flow over Florida, with a long fetch over the Atlantic Ocean. This long fetch is due to the position of the sub-tropical ridge, which is centered at approximately 31° N. The sub-tropical high pressure center at 700 mb (Fig. 9b) is further west (~67° W) than at 1000 mb, and shifted slightly to the south. The flow over Florida is more southerly as a result of this shift at 700 mb. This level also shows a long fetch over water, causing the PS nights to have the greatest mid-level moisture of all categories (64 percent, Table 2). The characteristics of this flow regime agree well with those of the Type A flow pattern

discussed by Reap (1994) and Type 1 pattern of Blanchard and Lopez (1985).

During OF flow the sub-tropical ridge axis at 1000 mb is south of the study area (Fig. 10a). This produces southwesterly flow over the peninsula. One should note the trough extending westward from the Carolinas to southern Arkansas. The location of this trough in conjunction with the sub-tropical ridge creates confluence of streamlines over the study area. The trough at 700 mb also exhibits a northeast to southwest orientation (Fig. 10b). Once again, there is confluence over Florida. Both charts suggest that air arriving over Florida originates from the tropics, while Table 2 indicates that OF flow has the second greatest mid-level humidity (60 percent). Reap (1994) found similar characteristics in the sea level pressure patterns of map Type B. The type 3 results of Blanchard and Lopez (1985) also agree with our findings.

Nights with CLM flow are characterized by southeasterly to southerly flow at 1000 mb along the east coast of Florida (Fig. 11a). The sub-tropical ridge axis is not well defined over Florida at this level. The ridge axis at 850 mb (not shown) is better defined and located directly over the study area. Thus, the air at this level experiences warming and drying due to subsidence associated with the ridge axis. At 700 mb, the flow is from the southwest in response to the stronger sub-tropical ridge axis located over South Florida (Fig. 11b). The air arriving over Central Florida at 700 mb does not appear to have a long fetch over water. As a result, the 700 – 500 mb layer relative humidity (55 percent) is less than the PS and OF flow regimes (Table 2).

In the ON regime, a trough at 1000 mb is present in the mid-latitudes of the Atlantic Ocean near 60° W (Fig. 12a). A center of high pressure can be seen just west of the trough east of the Virginia-North Carolina border. Examination of individual cases

b) 700 mb

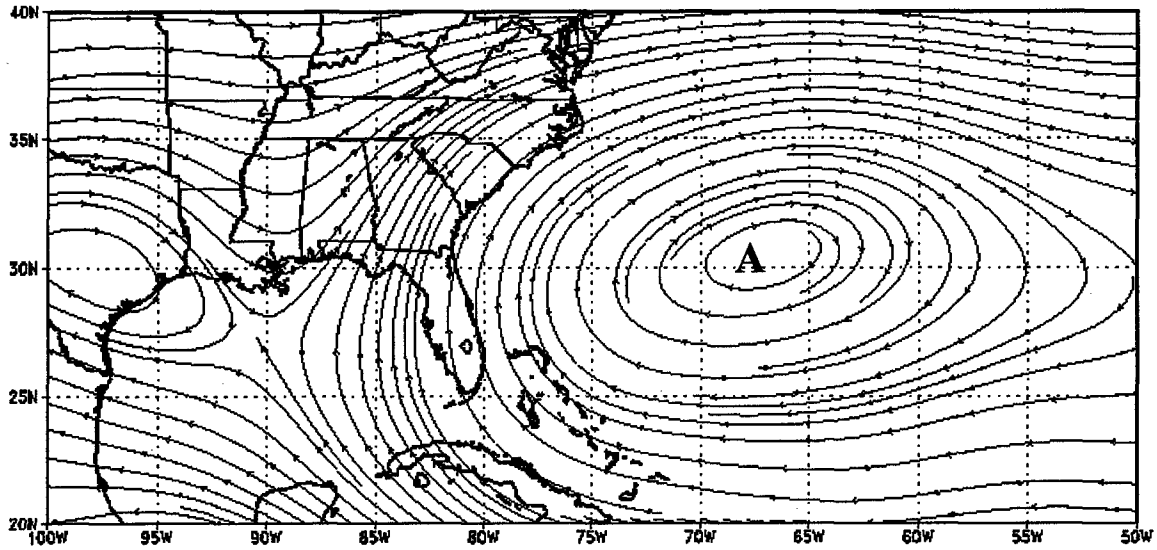

a) 1000 mb

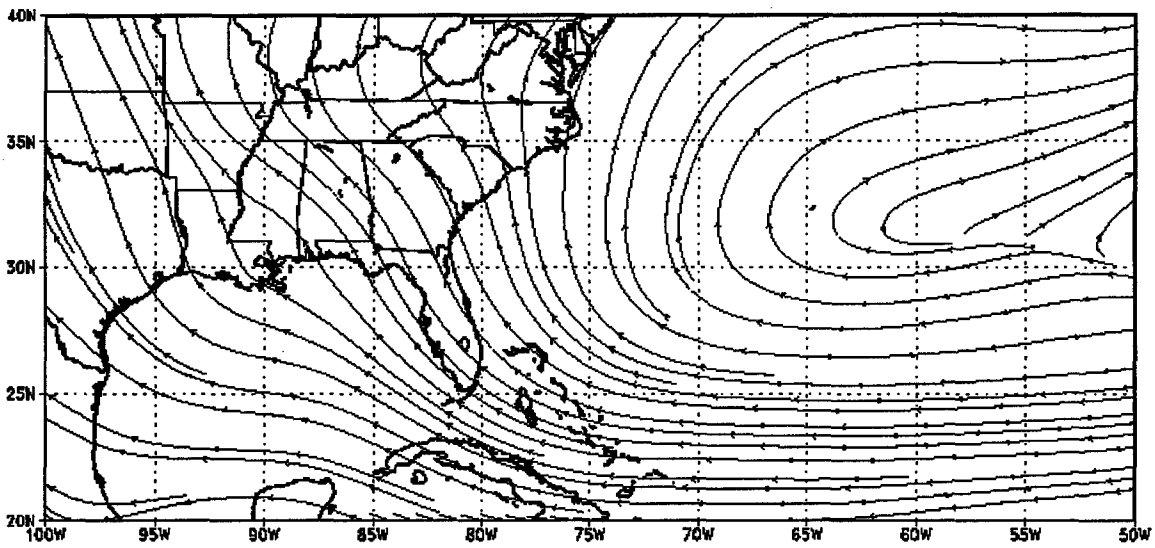

Fig. 9. Average streamlines for the PS regime at a) 1000 mb and b) 700 mb.

b) 700 mb

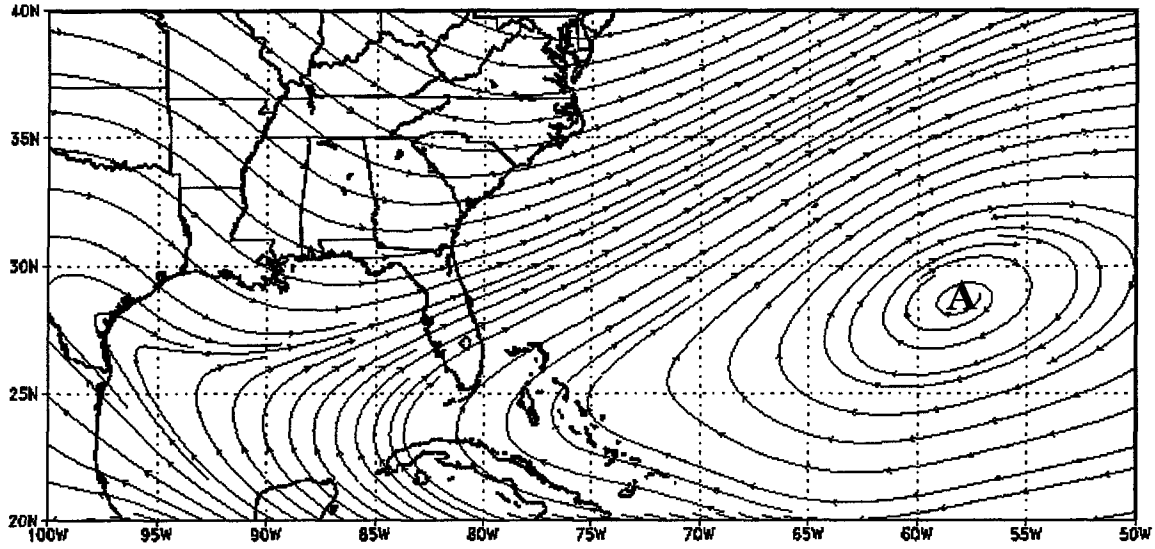

a) 1000 mb

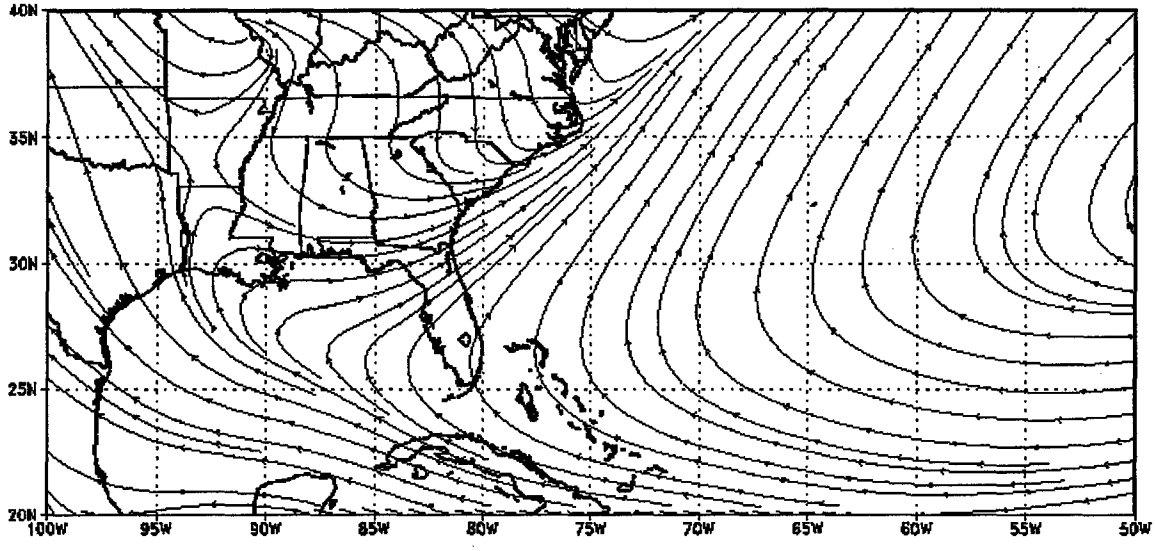

Fig. 10. Average streamlines for the OF flow regime at a) 1000 mb and b) 700 mb.

b) 700 mb

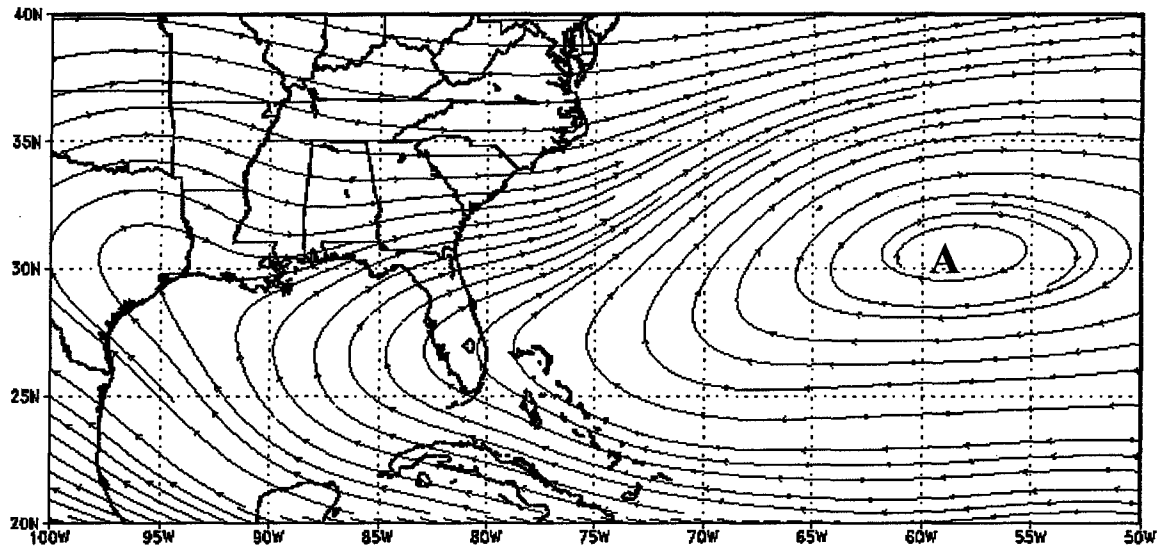

a) 1000 mb

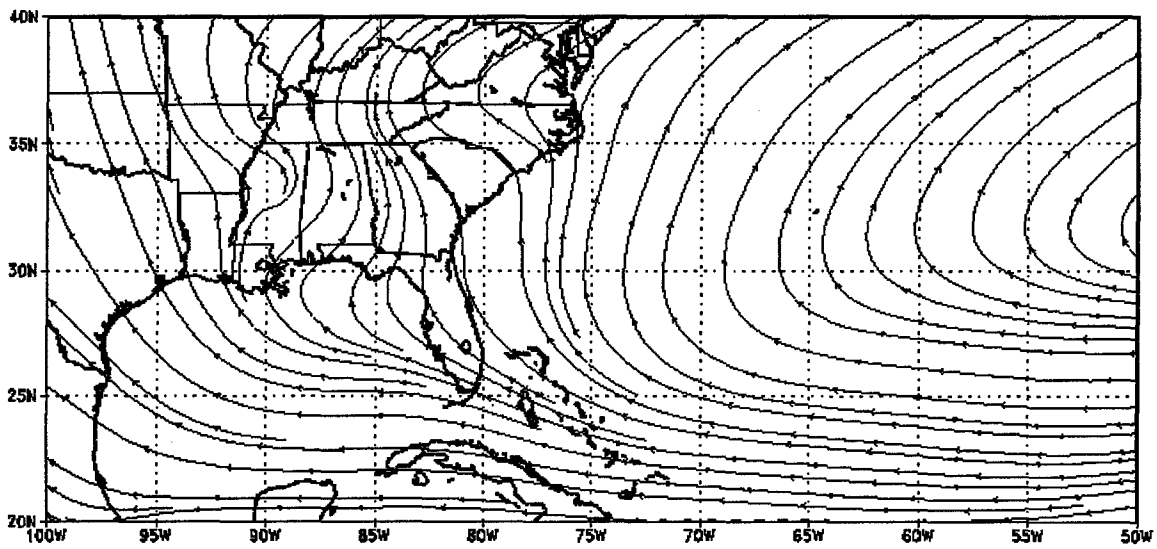

Fig. 11. Average streamlines for the CLM regime at a) 1000 mb and b) 700 mb.

b) 700 mb

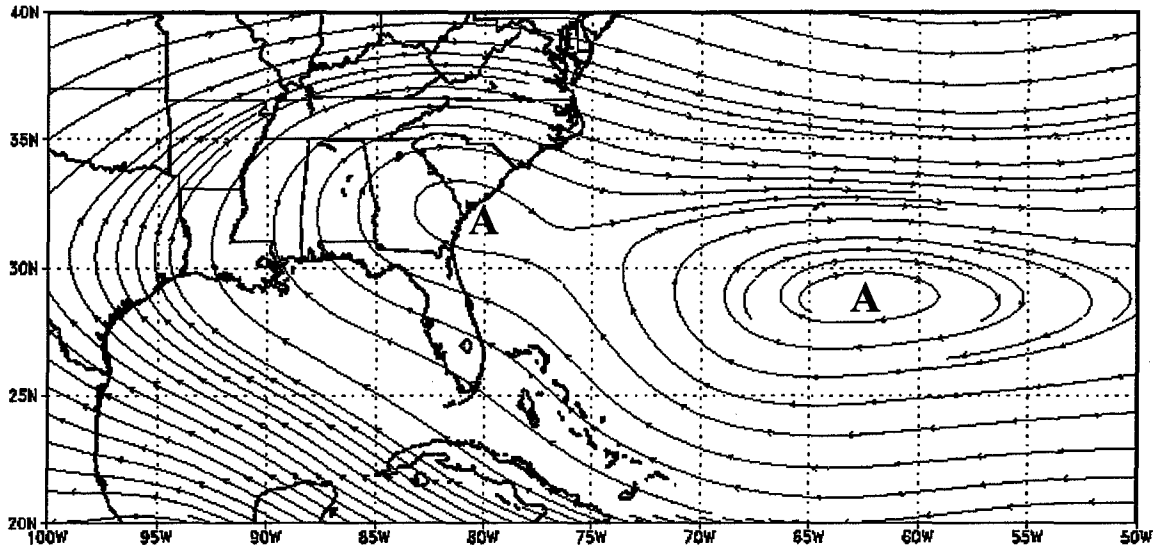

a) 1000 mb

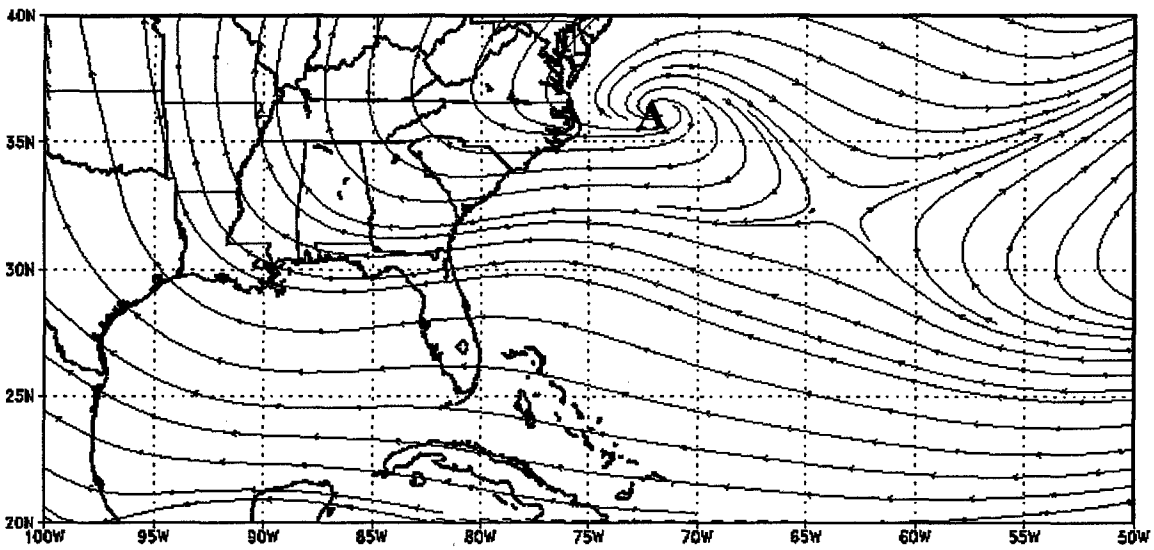

Fig. 12. Average streamlines for the ON regime at a) 1000 mb and b) 700 mb.

revealed that this area of high pressure was of continental origin. This pattern produces easterly flow over the study region, causing drier continental air associated with the mid-latitude high to be advected into the area. The 700 mb streamline analysis (Fig. 12b) shows more southeasterly flow. A weak area of high pressure off the coast of Georgia is an important feature at this level. Drier continental air associated with this high pressure system aids in reducing the moisture content at this level. The characteristics of this flow regime agree well with the characteristics of the Type C pattern discussed by Reap (1994) and Type 2 pattern discussed by Blanchard and Lopez (1985).

With a 700 – 500 mb layer relative humidity of 50 percent, the PN regime is the driest of our categories and has the smallest percent occurrence of CGL nights (50 percent) (Table 2). This flow regime is characterized by a well-defined northeast to southwest trough just off the East Coast (~ 25° N, 80° W to 40° N, 65° W) at 1000 mb (Fig. 13a). Northerly winds behind the trough bring dry continental air into the region. The well defined trough also is present at 700 mb (Fig. 13b). A high amplitude ridge is evident just west of the Mississippi River Valley. Northwest winds at this level reinforce the dry air at the lower level.

b) 700 mb

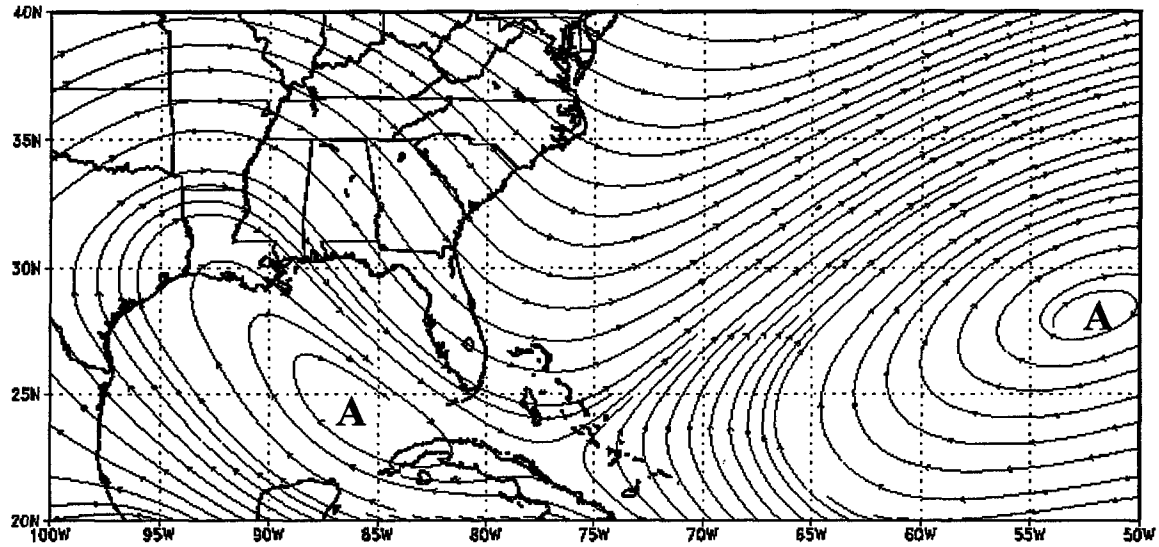

a) 1000 mb

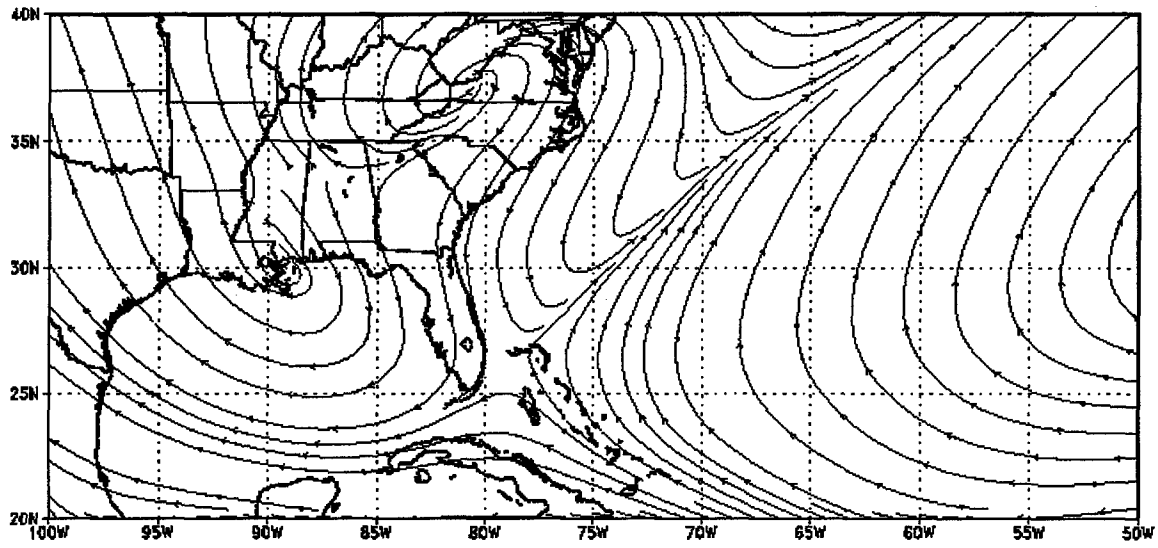

Fig. 13. Average streamlines for the PN regime at a) 1000 mb and b) 700 mb.

4. LOCAL NOCTURNAL THUNDERSTORM STUDY

An examination of Terminal Aerodrome Forecasts (TAFs) for the KSC Shuttle Landing Facility (KTTS) indicates that predicting nocturnal thunderstorms is a forecast challenge. For example, thunderstorms were forecasted to be in the vicinity of the SLF (within 40 km) on only 20 percent of the nights with CGL during weak synoptic scale forcing. Even more significant is the fact that 80 percent of these nights were not forecast to have thunderstorms. This indicates the need to develop forecast tools that better predict the onset of nocturnal thunderstorms. This section investigates several parameters for that purpose.

a. Thunderstorm Characteristics

As in the previously described lightning climatology, the CGL and NCGL nights were categorized into five wind regimes based on their 1000 – 700 mb mean vector wind (Fig. 14). The distribution of flow regimes in the local study is similar to that of the broader scale lightning climatology (refer to Chapter 3, Fig. 5). For example, OF flow days are most common, while CLM and PN regimes are least common. ON and PS flows also show a similar distribution to their corresponding regimes in the nocturnal lightning climatology, ranking second and third respectively. This similarity in flow distributions indicates that the nights in the local study are representative of the

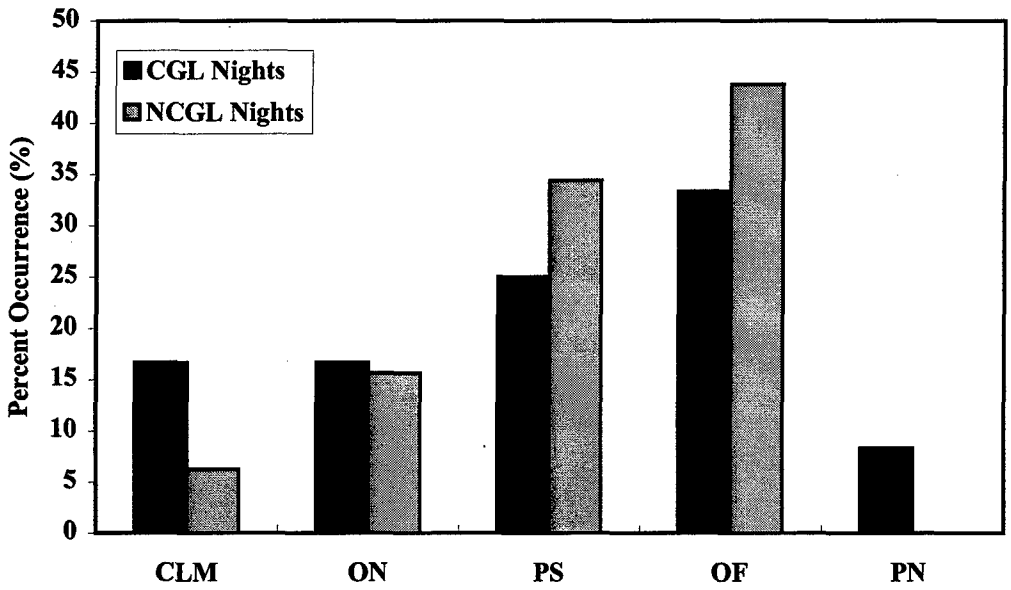

Fig. 14. Distribution of CGL and NCGL nights in the local study by wind regime.

larger population.

The nocturnal thunderstorm events were grouped according to surface synoptic features. Results reveal that the storms are most likely to occur in a high pressure synoptic environment (Table 4). Disturbed nights (36) account for 49 percent of the total. Stationary fronts are the most common disturbed feature (22 percent), while the effects of two tropical depressions and one hurricane contribute only slightly to nocturnal convection during the period of study.

Surface streamline analysis (Fig. 15) for the 36 disturbed CGL nights, 19 nights with CGL during weak synoptic scale forcing (case nights), and 32 nights without CGL during weak synoptic scale forcing (null nights), depict the differences in surface features of the three categories. On disturbed days (Fig.15a), the average position of the confluence zone associated with the stationary fronts, cold fronts and troughs extends northeastward from the southeast Gulf of Mexico over the peninsula of Florida into the Atlantic Ocean. This location indicates the role of fronts and troughs in the development of nocturnal thunderstorms over the Cape Canaveral area. On the other hand, the sub-tropical ridge is firmly established over the area of study on the case nights (Fig. 15b). The streamlines also indicate a trough over northern Georgia, Alabama, and Mississippi for this category. The streamline pattern for the null case nights is similar to that of the case nights with the sub-tropical ridge axis located over the Florida peninsula (Fig. 15c). The lack of surface synoptic scale forcing on case nights indicates that local and mesoscale features, combined with a favorable thermodynamic profile, is responsible for the initiation and development of nocturnal thunderstorms near Cape Canaveral.

Table 4. Surface synoptic conditions for nocturnal CGL events between 1995 – 1997. Percent occurrence of each synoptic condition is shown in parentheses.

Surface Synoptic Condition	Total	1995	1996	1997
High Pressure	38 (51)	11 (32)	18 (82)	9 (50)
Stationary Front	16 (22)	11 (32)	1 (5)	4 (22)
Trough	13 (18)	7 (21)	2 (9)	4 (22)
Cold Front	4 (5)	2 (6)	1 (5)	1 (6)
Tropical Depression	2 (3)	2 (6)	0	0
Hurricane	1 (1)	1 (3)	0	0
Total	74	34	22	18

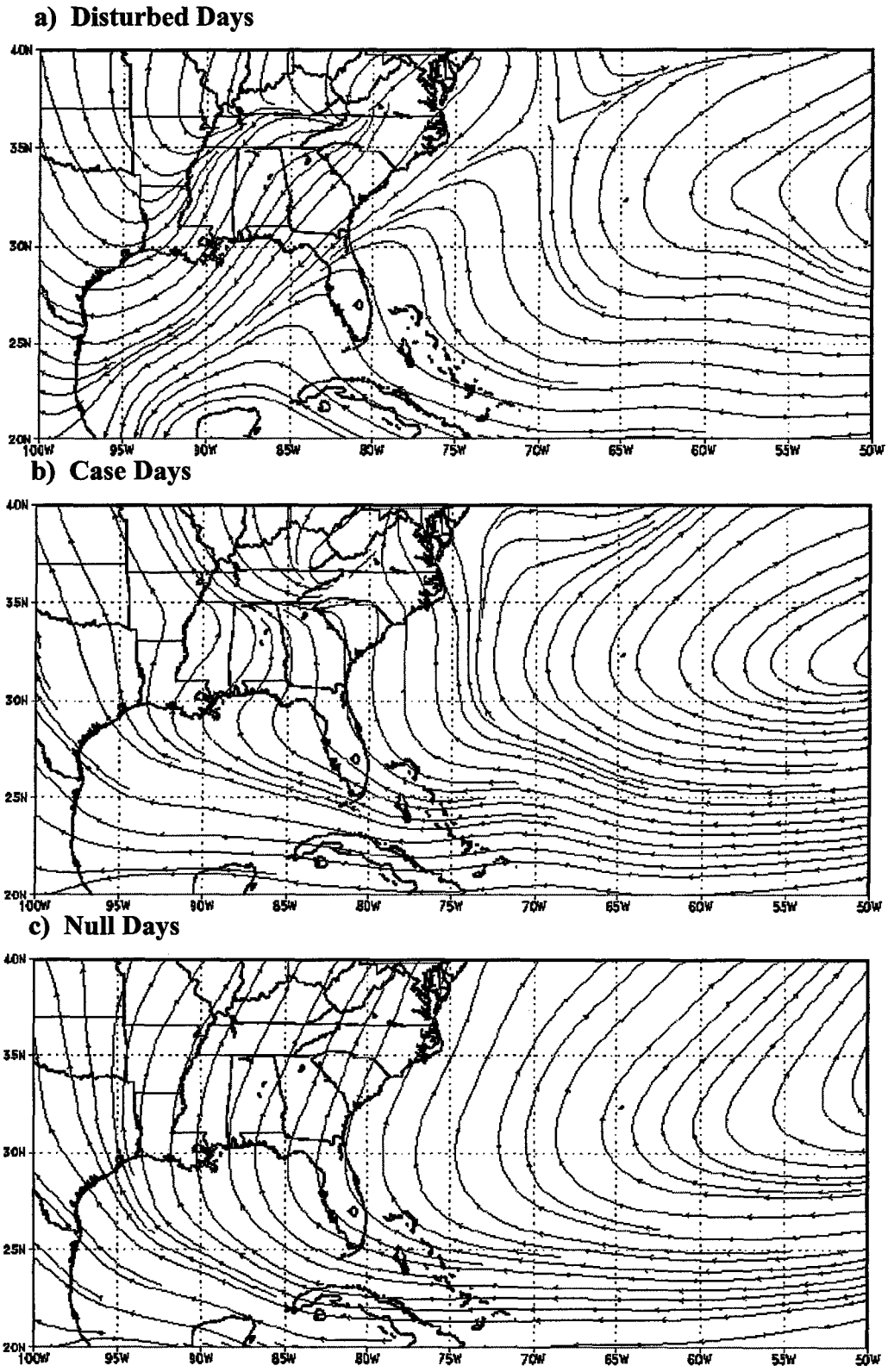

Fig. 15. Mean surface streamline analyses for a) disturbed days, b) case days, and c) null days.

b. Sounding Properties

Average CCAS evening soundings for the case days and null days (Fig. 16) show only a small contrast in temperature profiles. However, the dewpoint profiles exhibit a noticeable difference in the lower troposphere. The two categories also appear to have slight differences in wind direction at some levels. To investigate these differences, an analysis of individual vertical profiles of temperature, relative humidity, wind direction, and wind speed is presented.

1. Wind. Composite wind speed profiles at 2215 UTC (Fig. 17a) show little differentiation between case nights and null nights throughout the entire atmospheric column. The CGL and NCGL nights exhibit little vertical variability in speed below 600 mb, with the CGL nights having slightly weaker wind speeds. Above 600 mb, both CGL and NCGL show increasing speeds with height. The CGL category has stronger winds than the NCGL category in this layer. Again, the differentiation between the two categories above 600 mb is small. The greatest difference occurs at 200 mb; however, this difference is only 3 m s^{-1}. The remainder of the two profiles differs by 2 m s^{-1} or less. Lopez et al. (1984) found that lighter wind speeds were associated with increased convection.

The composite wind direction profile at 2215 UTC (Fig. 17b) indicates directional shear throughout the soundings of both the CGL and NCGL nights. Both the CGL and NCGL categories show veering winds from the southeast at 1000 mb to northwest at 200 mb. In general, differences between the two categories at a corresponding level are less than 30 degrees. The largest difference (40 degrees) occurs at 900 mb.

MRPP was performed on the wind speed, and u- and v-wind components to

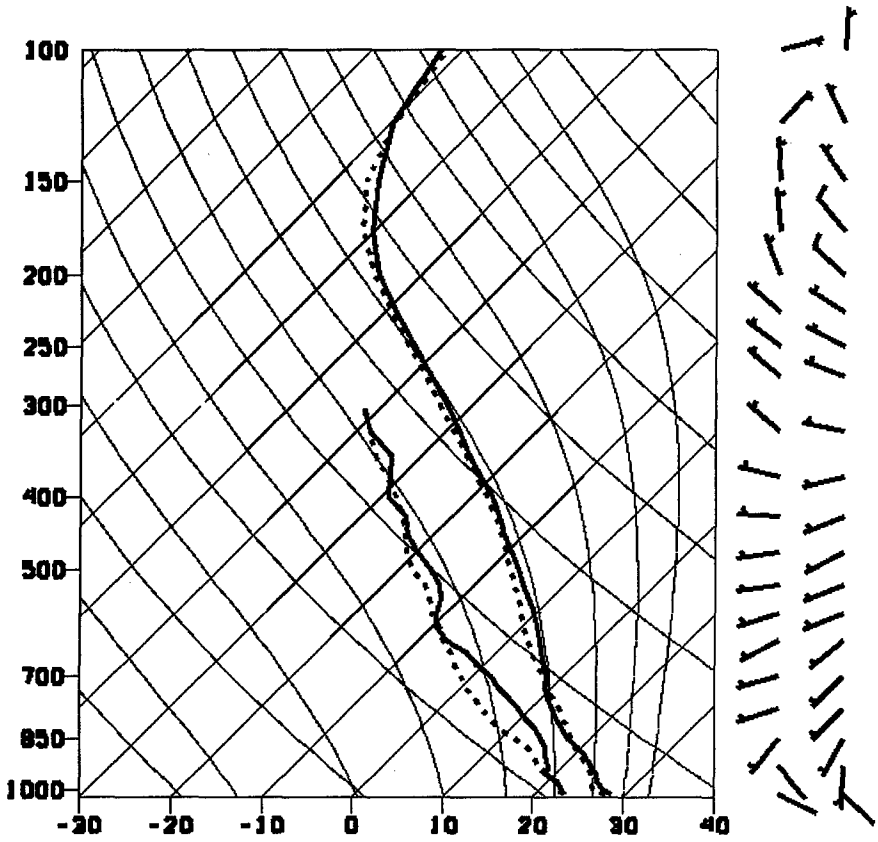

Fig. 16. Average evening CCAS soundings for CGL nights (solid) and NCGL nights (dashed). Case day winds are on the left-hand side of each sounding, with null day winds on the right. Small (large) wind barbs denote speeds of 2.5 m s^{-1} (5 m s^{-1}).

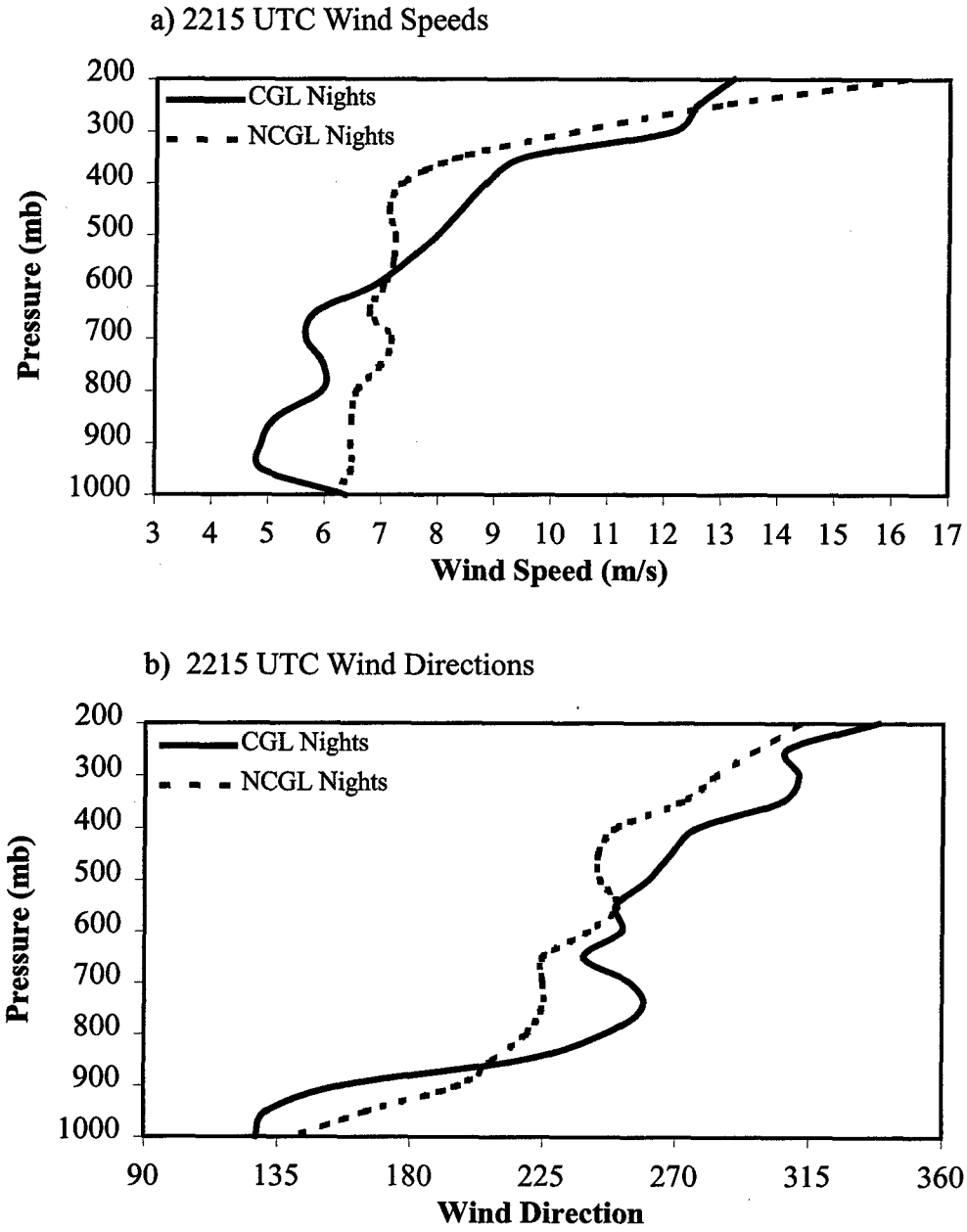

Fig. 17. Composite a) wind speed and b) wind direction profiles at 2215 UTC.

determine whether these parameters show statistically significant differences between convective categories. Results show that no wind parameter is significantly different at any level (no p-values ≤ 0.05). Wind speed best discriminates at 1000 mb (p-value = 0.1101). The *v*-wind component at 750 mb, however, is the best discriminator of all the wind parameters (a 0.0985 p-value). Wind speed at 750 mb also has a low, but not significant, p-value of 0.1158. The *v* component and wind speed at 750 mb wind, although they do not meet the 95% significance level, appear to be the best discriminators between CGL and NCGL nights. In summary, the collective results indicate that wind data are not good discriminators between CGL and NCGL nights.

2. Temperature. There is little obvious difference between the CGL and NCGL temperature profiles (Fig. 16). In order to reveal any subtle differences, the mean temperature profile of each category was subtracted from the mean temperature profile of all the soundings. These profiles for the CGL and NCGL nights are shown in Fig. 18a. The NCGL category shows less variation with height (0.56° C) than the CGL category (1.48° C). The maximum difference between categories (1.36° C) occurs at 600 mb. Except for the 850 – 700-mb layer, NCGL nights are cooler than CGL nights. MRPP significance tests confirm the lack of temperature distinction between nights with and without CGL flashes (not shown). These results are consistent with those of Kelly (1998) which showed a similar lack of distinction between temperatures at individual pressure levels for lightning days verses non-lightning days.

Two layers in the CGL profile exhibit large variations of temperature with height as compared to the corresponding layers in the NCGL profile (Fig. 18a): 1000 to 800 mb, and 800 to 600 mb. To understand better the temperature profiles in these layers,

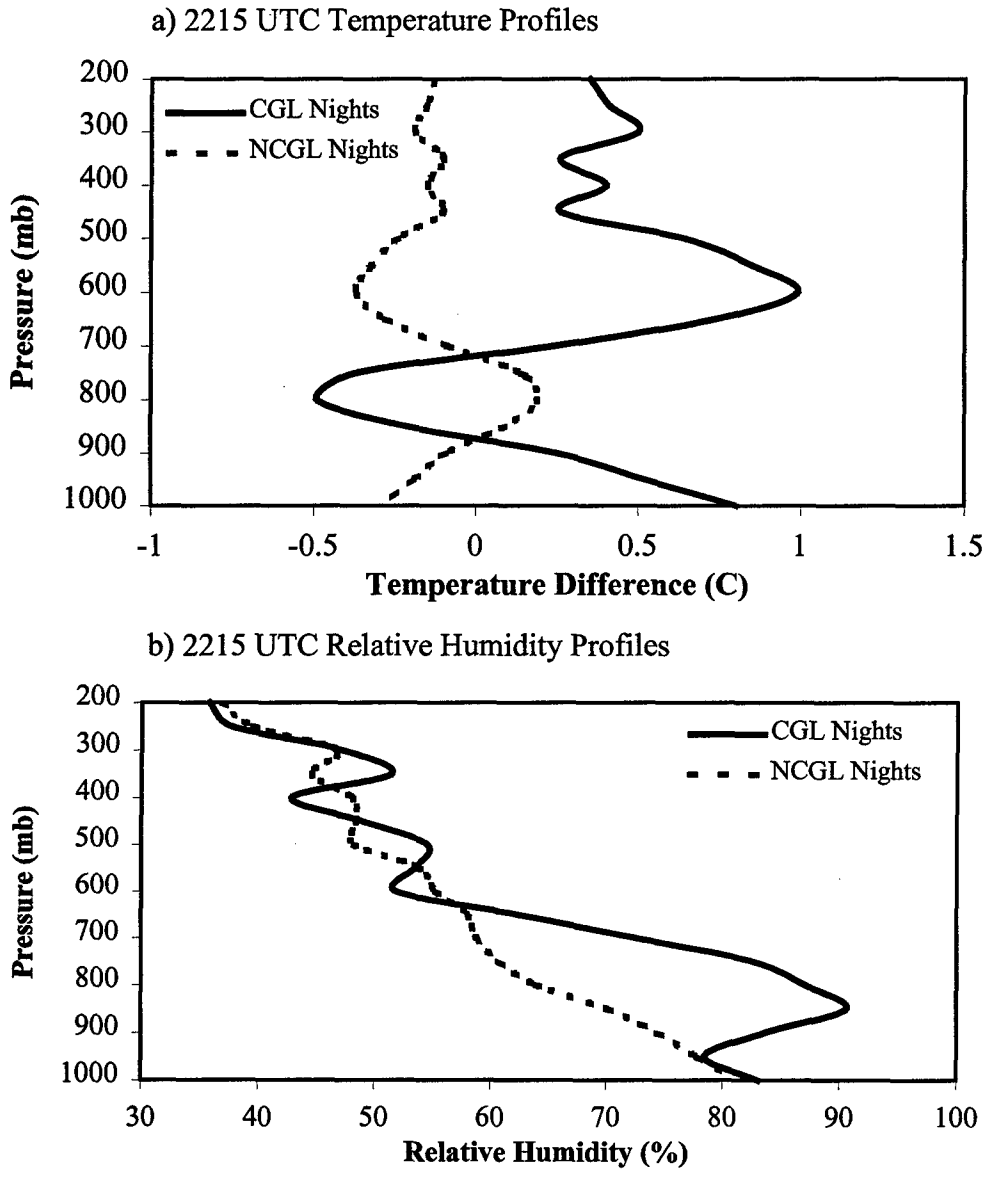

Fig. 18. Composite a) temperature and b) relative humidity profiles at 2215 UTC.

lapse rates in the 1000 to 800 mb and 850 to 500 mb layers were investigated.

Mean values of the 1000 – 800 mb mean lapse rate suggest that it might be good at differentiating CGL nights from NCGL nights (6.7°C km^{-1} for CGL nights versus 5.8°C km^{-1} for NCGL nights). The MRPP p-value of 0.0018 does indicate a significant difference between lapse rates of the two categories. To quantify the accuracy of a forecast based on this parameter, the TSS was calculated. A threshold of 6.59°C km^{-1} produces a TSS of 0.510 and a HSS of 0.497 (Table 5). POD, POFD, FAR, and CSI results for this predictor also are shown in Table 5.

In the 850 – 500 mb layer, mean lapse rates for the CGL (5.6°C km^{-1}) and NCGL (5.9°C km^{-1}) nights differ by only 0.3°C km^{-1}. These results suggest that this lapse rate does not provide good differentiation between categories. The MRPP test confirms that this lapse rate is not statistically significant at the 95 percent or higher confidence level (p-value=0.1198).

3. Relative Humidity. Vertical profiles of relative humidity (Fig. 18b) reveal moisture contrasts between the two categories. The profiles are almost identical below 950 mb, and above 600 mb the relative humidities show only small differences. Greatest differences occur in the 850 to 750 mb layer, where values for CGL nights average 20 percent greater than those of NCGL nights. The largest difference (23 percent) occurs at 800 mb where the relative humidity for CGL nights is 87 percent, and the NCGL average is 64 percent. The frequency distribution for relative humidity at 850 mb (Fig. 19a) indicates the differentiation between CGL and NCGL nights. The greatest occurrence of nights with CGL is associated with 850 mb relative humidities between 75 and 84 percent. The distribution for NCGL nights exhibits a broader range and generally lower

Table 5. Contingency tables for selected parameters based on data at 2215 UTC.

Predicted Category	CGL Event	NCGL Event	Total
1000 – 800 mb Lapse Rate			
≥ 6.59 °C/km	8	5	13
< 6.59 °C/km	4	27	31
Total	12	32	44
	POD = 0.667	POFD = 0.156	FAR = 0.385
	CSI = 0.471	TSS = 0.510	HSS = 0.497
850 mb RH			
≥ 77.4 %	10	8	18
< 77.4 %	2	24	26
Total	12	32	44
	POD = 0.833	POFD = 0.250	FAR = 0.444
	CSI = 0.500	TSS = 0.583	HSS = 0.505
850 – 700 mb RH			
≥ 70 %	10	8	18
< 70 %	2	24	26
Total	12	32	44
	POD = 0.833	POFD = 0.250	FAR = 0.444
	CSI = 0.500	TSS = 0.583	HSS = 0.505
K-Index			
≥ 31 °C	10	13	23
< 31 °C	2	19	21
Total	12	32	44
	POD = 0.833	POFD = 0.406	FAR = 0.565
	CSI = 0.400	TSS = 0.427	HSS = 0.332
Modified K-Index			
≥ 18.2 °C	12	8	20
< 18.2 °C	0	24	24
Total	12	32	44
	POD = 1.000	POFD = 0.250	FAR = 0.400
	CSI = 0.600	TSS = 0.750	HSS = 0.621

a) 850 mb RH

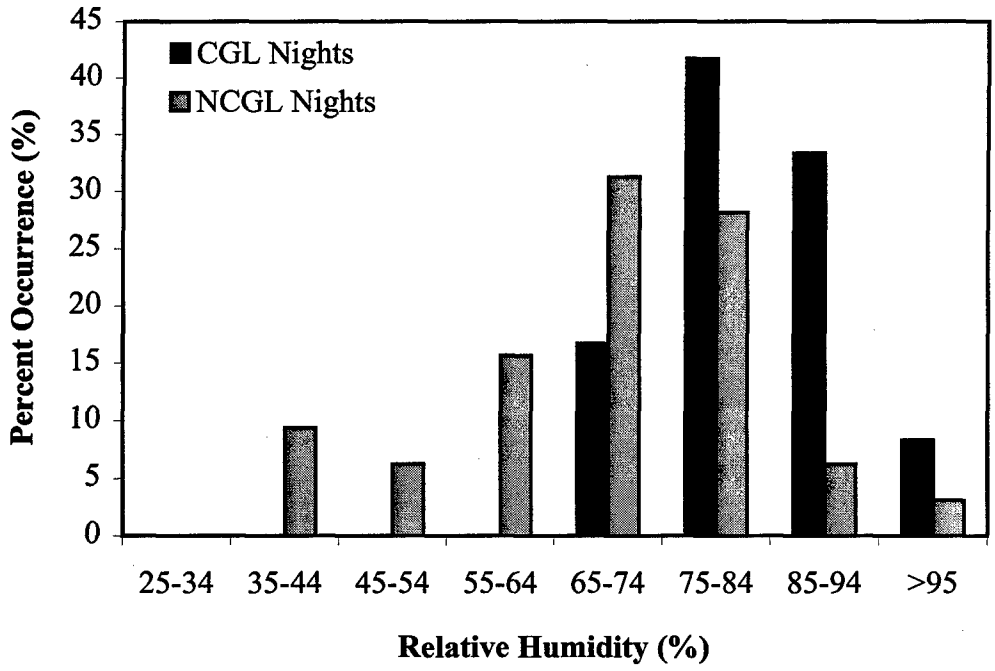

b) 850 – 700 mb RH

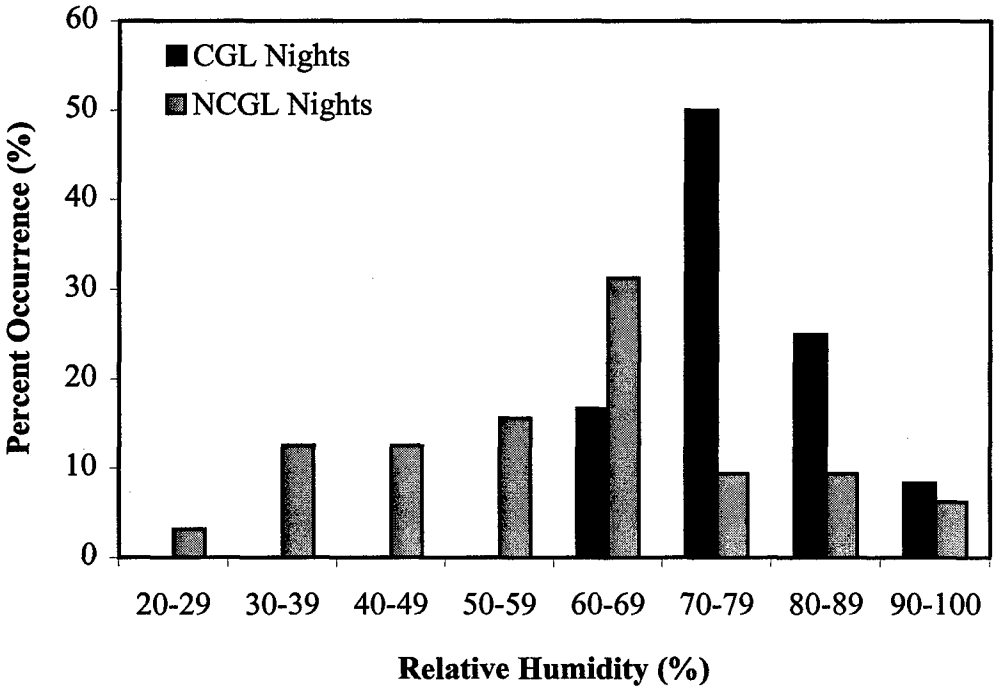

Fig. 19. Frequency distributions for a) 850 mb RH and b) 850 – 700 mb RH at 2215 UTC.

values.

Relative humidities at the 850, 800 and 750 mb levels show statistical significance in discriminating between CGL and NCGL nights. P-values are 0.0217 and 0.0127 for the 750 and 800 mb levels, respectively. The 850 mb p-value of 0.0007 shows the best discrimination of the three levels. This level also exhibits the greatest forecast skill. Based on a threshold of 77 percent, the 850 mb relative humidity produces a TSS of 0.583 (HSS = 0.505) (Table 5). These results are better than those of Kelly (1998) where the 700 mb relative humidity produced a 0.47 TSS for forecasting lightning days verses non-lightning days near Cape Canaveral.

The good differentiation between categories by the 850 to 700 mb layer requires further investigation. The average relative humidity in this layer for CGL nights is 76 percent, with the NCGL nights having a relative humidity of 60 percent. The frequency distribution (Fig. 19b) shows that 50 percent of the CGL nights have relative humidity values between 70 and 79 percent, while only 9 percent of the NCGL nights have relative humidity values in this range. The MRPP value of 0.0081 indicates a statistically significant difference between categories. The TSS for this layer is 0.583 (HSS = 0.505), based on a 70 percent threshold (Table 5). This TSS score is equal to that of 850 mb relative humidity.

4. Stability. MRPP p-values, means, maximam, minimam, and standard deviations for the eight stability parameters that were examined are shown in Table 6. Differences in means between categories, though small, show that the CGL nights are less stable, and therefore more favorable for convection. However, LI and LFC have equal means for the CGL and NCGL nights. MRPP values indicate that a majority of the

stability parameters do not show significant differences between categories. CIN is the worst discriminator with a p-value of 1.0000. Conversely, the Showalter and K-Indices are the best discriminators, with p-values of 0.0201 and 0.0256 respectively.

In terms of forecast skill, the Showalter Index does not appear to be useful for discriminating between CGL versus NCGL nights. For example, frequency distributions of the Showalter Index (not shown) for the CGL and NCGL nights are similar. The forecasting score for the Showalter Index also is low, i.e., a threshold of 0° C produces a TSS of only 0.29, as compared to the 0.583 score for 850 mb and 850 – 700 mb relative humidity.

Frequency distributions of the K-Index indicate that 67 percent of CGL nights have values between 31 – 35° C, while only 31 percent of NCGL nights are in the same range (Fig. 20a). The K-Index shows the best forecast skill of all the standard stability parameters (TSS = 0.427 and HSS = 0.332) (Table 5). This TSS score is less than the 0.583 of the 850 mb and 850 – 700 mb relative humidity, but greater than that of the Showalter Index (0.290). These results also are better than those of Fuelberg and Biggar (1994) where the K-Index produced a 0.19 TSS for forecasting strong convective days versus weak or non-convective days in the Florida panhandle.

The K-Index is defined as:

$$KI = (T_{850mb} - T_{500mb}) + TD_{850mb} - TDD_{700\ mb},$$

where TD is the dewpoint temperature and TDD is the dewpoint depression. The K-Index considers thunderstorm potential based on temperature lapse rate between 850 and 500 mb and moisture content from 850 to 700 mb. One should recall that the 850 – 500

Table 6. Statistics describing stability parameters at 2215 UTC.

Index and Category	MRPP p-values	Mean	Maximum	Minimum	Standard Deviation
K Index	0.0256				
CGL		33	38	26	3
NCGL		28	39	4	7
Modified K Index	0.0006				
CGL		22	28	18	3
NCGL		14	26	-8	8
Lifted Index	0.6467				
CGL		-3	-1	-7	2
NCGL		-3	1	-7	2
Showalter Index	0.0201				
CGL		-1	2	-4	2
NCGL		1	10	-3	3
Total Totals	0.2923				
CGL		46	50	43	2
NCGL		45	50	32	3
CAPE	0.7552				
CGL		1701	3357	331	1010
NCGL		1665	3693	0	1090
CIN	1.0000				
CGL		57	157	0	48
NCGL		69	356	0	72
LFC	0.4615				
CGL		821	961	549	108
NCGL		821	1017	439	97

a) K-Index

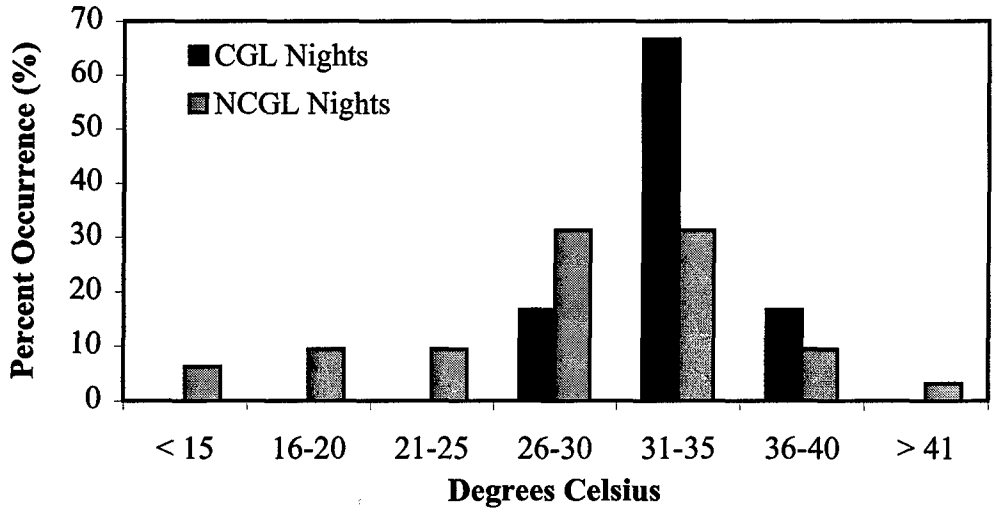

b) Modified K-Index

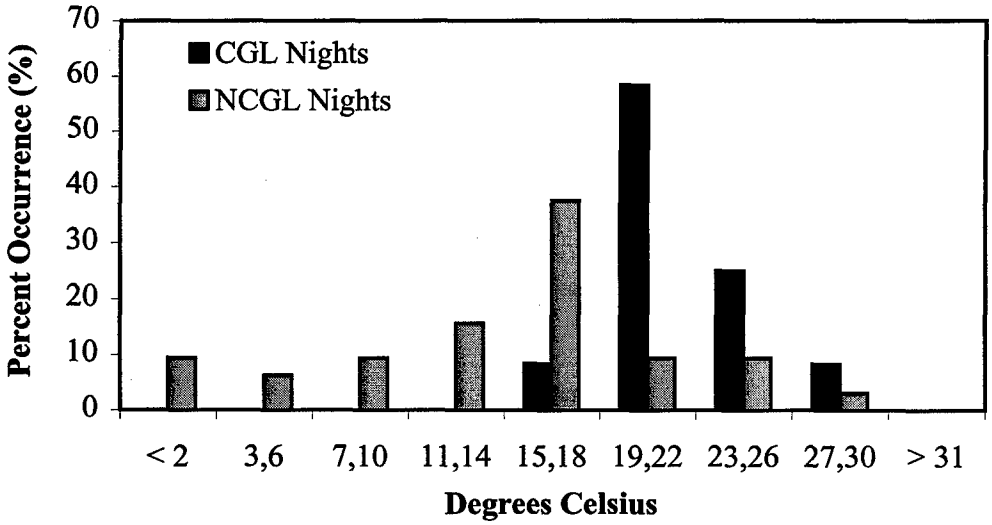

Fig. 20. Frequency distributions for a) K-Index and b) modified K-Index.

mb lapse rate was not found to be a statistically significant discriminator, whereas the 850 – 700 mb relative humidity was found to be statistically significant. These findings indicate that moisture provides the main contribution to the statistical significance of the K-Index.

The previous discussion on lapse rate indicated that the 1000 – 800 mb lapse rate was statistically significant discriminator, whereas, the 850 – 500 mb lapse rate was not (p-value of 0.0018 versus 0.1198). Taking advantage of this finding, and the statistical significance of the 850 – 700 mb relative humidity, we replaced the 850 – 500 mb temperature difference with the 1000 – 800 mb temperature difference in the K-Index. Thus, the modified K-Index is defined as:

$$KI = (T_{1000mb} - T_{800mb}) + TD_{850mb} - TDD_{700\ mb}.$$

The frequency distribution of the Modified K-Index (Fig. 20b) shows better differentiation than the corresponding distribution for the original K-Index (Fig. 18a), e.g., 58 percent of CGL nights have modified K Indices between 19 – 22° C, while only 9 percent of NCGL nights are in the same range. MRPP results show that of all the parameters investigated, the modified K-Index is the best at discriminating between CGL and NCGL nights (p-value = 0.0006). It also produces the highest TSS score of 0.750 (HSS = 0.621) based on a threshold of 18.2° C (Table 5), a 0.323 increase over the K-Index.

To confirm the optimum thresholds for the predictors in Table 5, 5000 samples based on the original, were generated using a bootstrap method. A histogram showing the distribution of thresholds that produced the greatest TSS for the Modified K-Index is shown in Fig. 21. The Modified K-Index value of 18.2 °C km^{-1} produces the greatest

TSS in 61 percent of the 5000 samples. These results confirm our threshold found using the original sample. Histograms (not shown) confirm the optimum thresholds for the remaining four predictors. These results suggest that the combination of low level instability and mid-tropospheric moisture is the best predictor of nocturnal thunderstorms that occur under weak synoptic forcing.

c. Mechanisms Initiating Convection

Land-sea temperature differences during the warm season produce a horizontal temperature gradient that forces daily sea breeze circulations. These circulations act as the main trigger mechanisms for convective initiation during the afternoon and early evening hours. However, as the sun sets, the solar insolation decreases. The horizontal temperature gradient then reverses, and a nighttime land breeze circulation is established that is weaker than the daytime sea breeze. The lack of solar insolation during the night, and the weaker vertical velocities associated with the land breeze circulation, result in diminished convective initiation during situations of weak synoptic scale forcing. Mechanisms leading to nocturnal convective initiation were examined using 0.5° base reflectivity data from the WSR-88D at the National Weather Service Office Melbourne, Florida.

The radar imagery showed that convective initiation occurs over water on 42 percent of the 19 nights with CGL, with the greatest incidence of oceanic initiation occurring during parallel flow from the south. The imagery revealed no observable convergence boundaries over water on these nights. Storms typically form over the relatively warm waters of the Gulf Stream and then are advected into the area of study by

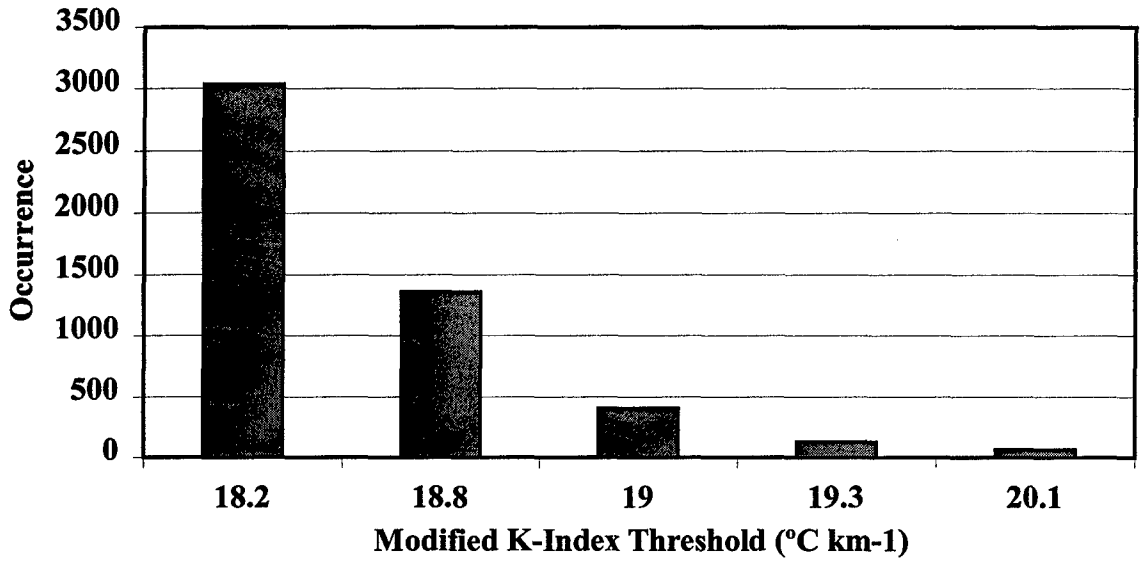

Fig. 21. Histogram showing the distribution of Modified K-Index thresholds that produce the greatest TSS.

the southerly flow. As the storms move over land, they begin to weaken and soon diminish. The average initial CGL flash for these storms is 0700 UTC. These observations suggest that thunderstorm initiation over the Atlantic Ocean is a result of low-level instability. This instability is created because air near the surface mirrors the almost constant temperature of the water, while radiative cooling produces colder temperatures aloft.

The various stages of a storm that formed over water on 18 August 1996 are shown in Fig. 22. The first radar image (0847 UTC) shows the storm beginning to develop southeast of Cape Canaveral (Fig 22a). During the next 30 minutes the convection strengthens as it moves northwest. By 0916 UTC (Fig. 22b) the storm is in its mature stage and begins to dissipate as it approaches the coast. The remnants of the storm can be seen off the coast of the city of Cape Canaveral at 0945 UTC (Fig. 22c). No evidence of the storm remains in the final radar imagery (1014 UTC, Fig. 22d). The storm produced a single flash at 0910 UTC.

Outflow boundaries produced by late afternoon and early evening thunderstorms are a second triggering mechanism indicated by the radar imagery. This mechanism occurs on 26 percent of CGL nights. These boundaries are most evident during calm flow, i.e., 1000 – 700 mb mean vector wind speeds less than 2 m s^{-1}. The outflow boundaries develop as the cool downdraft air from a thunderstorm hits the ground and spreads out horizontally. The current radar imagery showed that most of the outflow boundaries are produced by inland thunderstorms. As the night progress, the boundaries propagate eastward and initiate convection over the study area. The initial CGL flash associated with these storms occurs earlier (0253 UTC) than CGL flashes produced by

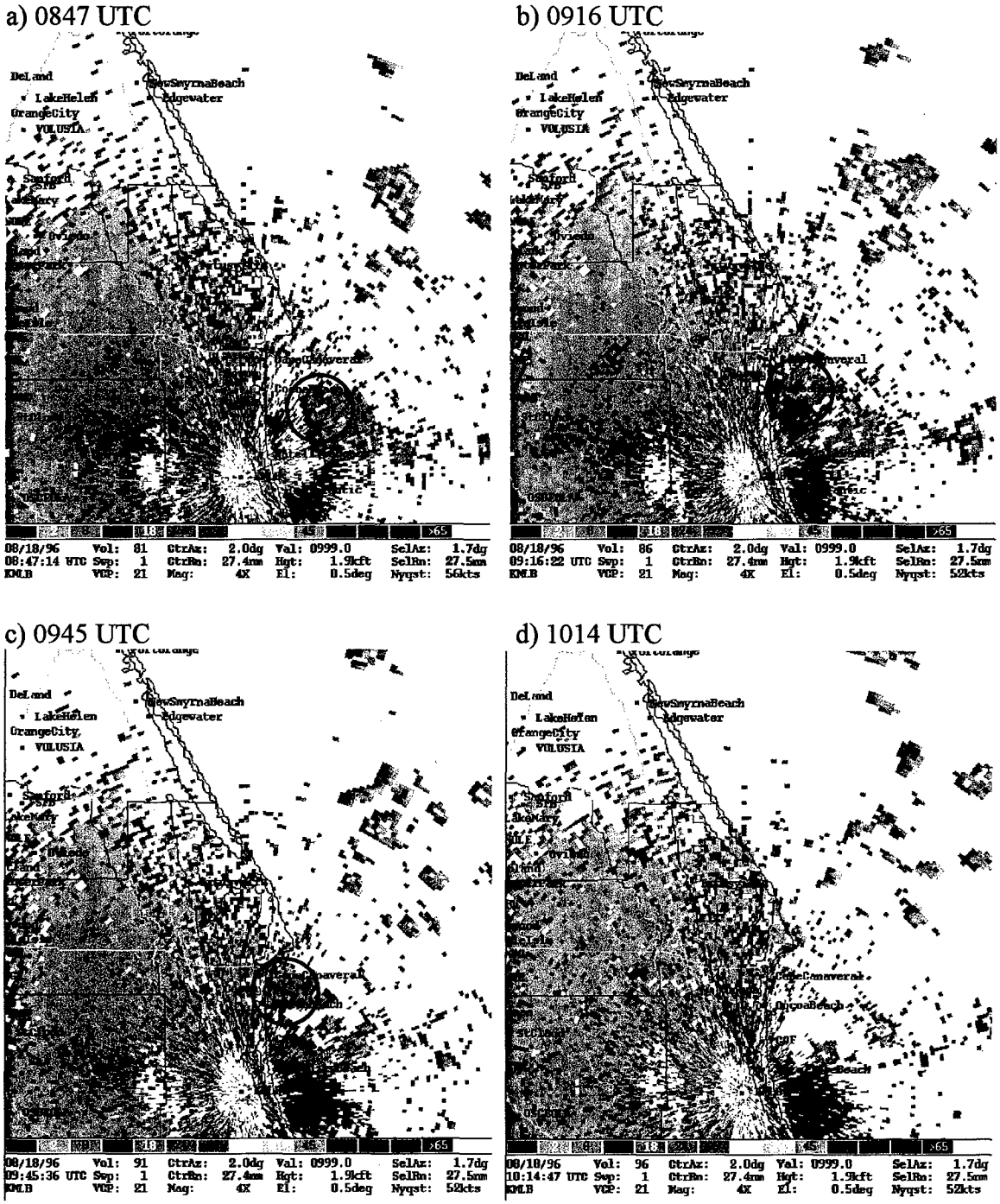

Fig. 22. Radar indicated thunderstorm (circled) that forms over water at a) 0847 UTC and b) 0916 UTC and then dissipates as it moves toward Cape Canaveral at c) 0945 UTC and d) 1014 UTC on 18 August 1996.

storms that formed over the water (0700 UTC).

An example of an outflow boundary initiating convection over the study area is shown in Fig 23. Radar imagery at 0217 UTC (Fig. 23a) shows an eastward moving outflow boundary produced by a thunderstorm to the west of the Kennedy Space Center. During the next 50 minutes the boundary continues its eastward progression, and triggers convection as it reaches the western shore of Merrit Island. This convection produces its first flash at 0303 UTC. By 0307 UTC (Fig. 23b) the thunderstorm triggered by the outflow boundary is clearly seen over Merrit Island. After producing 5 flashes, the storm quickly dissipates, producing its last flash at 0316 UTC.

No observable mechanism for convective initiation could be found on 32 percent of the nights with CGL. During these cases the greatest incidence of initiation occurs during offshore flow. The average time of the initial CGL flash is 0508 UTC. Further investigation of these nights, as well as nights when thunderstorms form either over water or as a result of outflow boundaries, is needed.

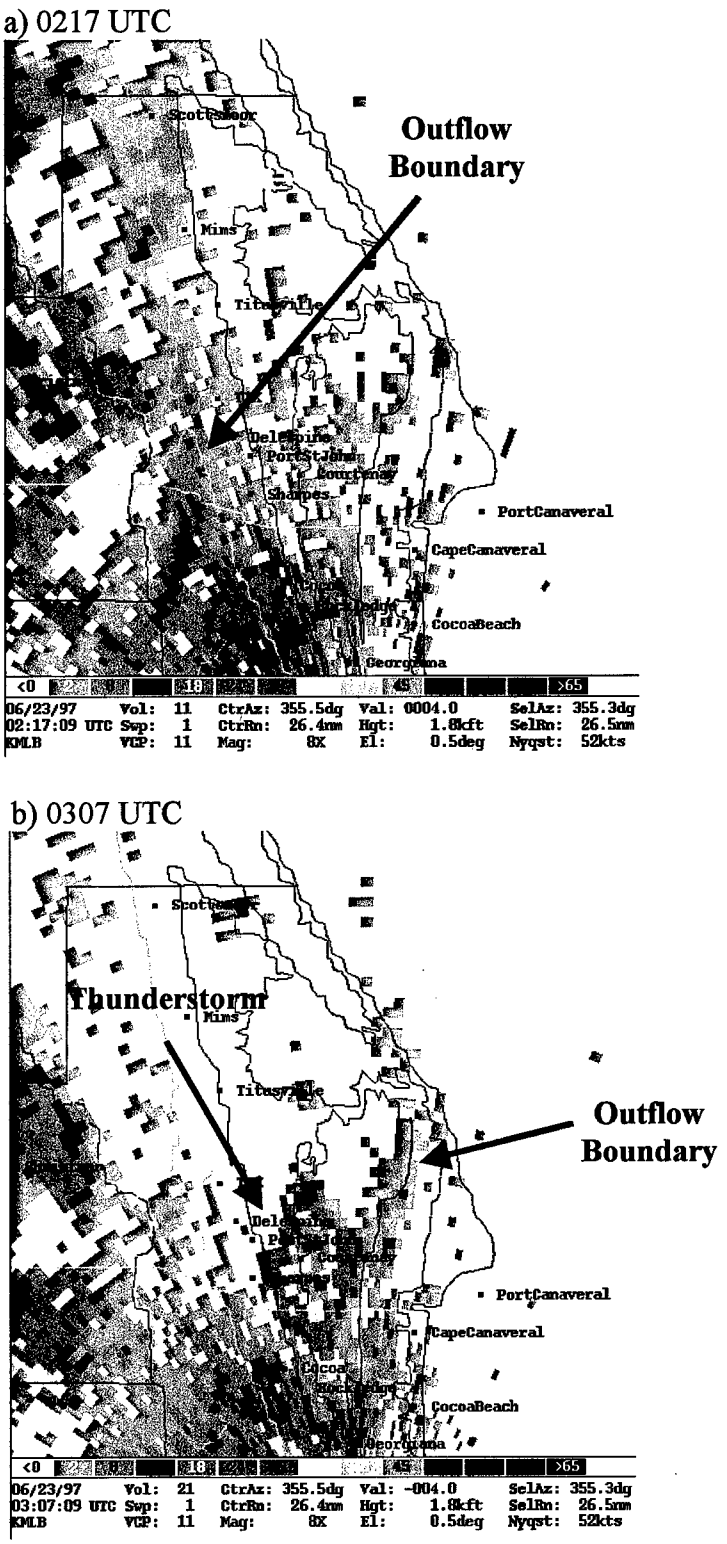

Fig. 23. Outflow boundary indicated by radar imagery at a) 0217 UTC and b) 0307 UTC that produces a thunderstorm over the study area on 23 June 1997.

5. SUMMARY AND CONCLUSION

This study has examined two aspects of nocturnal convection over Florida: A climatology of warm season nocturnal CGL flashes over east central Florida, and warm season nocturnal thunderstorms that develop near Cape Canaveral, Florida. Nocturnal thunderstorms that develop during undisturbed synoptic conditions were studied in detail because they are difficult to forecast. They form over the KSC/CCAS with little or no warning. Our goal was to provide information to the 45 WS that would increase their understanding of nocturnal thunderstorms in their area of forecast responsibility and the surrounding area.

a. Nocturnal CGL Flash Climatology

Seven years of warm season radiosonde data (1992 – 1998) were used to categorize nights into one of five wind regimes based on the 1000 – 700 mb mean vector wind. Data from the National Lightning Detection Network (NLDN) then were examined to determine nights that experienced CGL flashes. Nocturnal lightning was defined to occur between 0200 to 1300 UTC. Flashes were found on 64 percent of the nights that had available soundings (525 nights). Spatial maps of CGL flashes were constructed for each of the five wind categories. Most nocturnal lightning was found to occur over the warm Gulf stream waters just east of Cape Canaveral. CGL flash statistics

for the categories were compared to values of lapse rate and moisture. Streamline analyses described flow patterns for the five wind regimes.

Flow parallel to the peninsula from the south was found to have the greatest percent occurrence of nights with CGL flashes, although it had only the fourth greatest number of strikes. Findings indicated that enhanced midlevel moisture (700 – 500 mb) increased the percent occurrence of nights with CGL flashes. Current results agree with previous studies of convection over the Florida peninsula (e.g., Burpee 1979; Lopez et al. 1984; Watson et al. 1991). Midlevel lapse rates (850 – 500 mb) also were investigated. However, the lapse rates varied little between categories, and the more unstable midlevel lapse rates did not increase the likelihood of nocturnal CGL flashes. Streamline analyses revealed that differences in synoptic flow explain the thermodynamic characteristics of air flowing over our study area. The number of CGL flashes also is influenced by differences in the synoptic flow.

b. Local Nocturnal Thunderstorm Study

Nocturnal CGL flashes were found on 74 nights during the warm season months of 1995 – 1997 based on the local lightning detection system operated by KSC. NCEP surface analyses maps were examined to eliminate nights with disturbed flow, while WSR-88D data were analyzed to eliminate pre-existing convection. This screening left 19 nights with CGL that developed under weak synoptic scale forcing. A null data set containing 32 undisturbed nights without CGL flashes was chosen to compare atmospheric and stability parameters between the two data sets. A statistical comparison of stability, temperature, wind, and moisture parameters between the categories was

conducted using Multi-Response Permutation Procedures (MRPP). Forecast skill of the parameters that were found to be statistically significant was calculated using True Skill Statistic (TSS), Heidke Skill Score (HSS), and the Critical Success Index (CSI).

Wind speed and *u*- and *v*-wind components did not statistically discriminate between nights with or without CGL. However, the 750 mb wind speed and *v*-wind component were best at showing statistical discrimination.

Temperatures at individual levels also did not show statistically significant differences. Lapse rates in the 1000 – 800 mb and 850 – 500 mb layers were statistically evaluated using MRPP. Only the 1000 – 800 mb lapse rate statistically discriminated between the two categories. This low level lapse rate also showed good forecasting skill.

Relative humidity at the 850, 800, and 750 mb levels all showed statistical significance in discriminating between categories. Of these three levels, relative humidity at 850 mb was the best discriminator. The 850 mb relative humidity exhibited better forecast skill than the 1000 – 800 mb lapse rate. The 850 – 700 mb layer averaged relative humidity also indicated statistical significance. This layer showed identical forecasting skill to the 850 mb relative humidity.

Only two stability parameters (K-Index and Showalter Index) exhibited statistically significant discrimination between CGL and NCGL nights. However, the Showalter Index did not show good forecasting skill. The K-Index showed a greater forecast skill than the Showalter Index.

A Modified K-Index was created using the 1000 – 800 mb lapse rate and the 850 – 700 mb moisture. This new index showed the best statistical discrimination and forecast skill of all the parameters examined. The forecasting skill of the Modified K-

Index exhibited an increase over the forecasting skill of the standard K-Index. It also showed an increase in forecasting skill over that of the 850 mb relative humidity and 850 – 700 mb mean relative humidity.

An examination of radar imagery revealed that the greatest incidence of thunderstorm initiation (42 percent) occurred over the Gulf Stream with the most common wind direction being southerly flow parallel to the peninsula. Outflow boundaries were responsible for thunderstorm initiation on 26 percent of nights with CGL, occurring mainly during calm flow. No identifiable forcing mechanism in the radar imagery could be found on 32 percent of CGL nights.

This study has documented the climatology of warm season nocturnal CGL flashes over east central Florida. It also has examined warm season nocturnal thunderstorms that develop near Cape Canaveral, Florida. The parameters found to have the greatest forecast skill should be helpful in predicting nocturnal thunderstorms that develop over KSC/CCAS on nights with weak synoptic forcing. Further research is needed to assess the forecasting skill of the combination of these parameters. It is also clear that mesoscale modeling is needed to better identify additional mechanisms that are beyond the scope of this research.

APPENDIX

Table A1. Values of the CGL significant parameters from the 2215 UTC sounding used to calculate TSS, HSS, and CSI.

Date	850 mb RH	850 – 700 mb RH	K-Index	Modified K-Index	1000 – 800 mb Lapse Rate
30 May 95	80.5	76	33	20.7	6.35
16 Jul 95	66.0	64	33	18.2	6.22
28 Jul 95	94.3	70	26	20.1	8.52
18 Jun 96	89.8	75	34	19.0	5.64
22 Aug 96	77.4	75	29	20.3	8.04
28 Aug 96	74.1	83	36	24.5	6.70
5 Sep 96	92.1	83	33	24.7	7.14
6 Sep 96	94.5	84	35	24.6	6.59
9 Sep 96	78.7	79	32	18.8	5.32
7 Jul 97	77.6	70	33	19.3	6.84
18 Aug 97	92.7	92	38	27.8	6.78
24 Sep 97	79.0	64	31	20.1	6.65

Table A2. Values of the NCGL significant parameters from the 2215 UTC sounding used to calculate TSS, HSS, and CSI.

Date	850 mb RH	850 – 700 mb RH	K-Index	Modified K-Index	1000 – 800 mb Lapse Rate
17 May 95	68.1	35	22	6.0	5.30
18 May 95	81.1	54	26	14.8	7.35
31 May 95	79.5	92	39	26.4	6.60
7 Jun 95	73.4	36	20	6.9	5.47
23 Jun 95	62.9	64	31	14.2	4.35
26 Jun 95	95.0	84	36	21.4	5.24
27 Jun 95	75.6	45	25	11.1	6.01
3 Jul 95	34.9	29	15	-1.7	5.39
14 Jul 95	74.6	70	33	19.3	5.98
26 Jul 95	84.8	91	39	25.5	5.43
27 Jul 95	62.7	65	30	15.5	5.35
13 Sep 95	50.2	59	27	13.2	6.37
13 Jun 96	75.0	64	27	13.2	6.35
14 Jun 96	85.1	59	29	15.0	6.23
19 Jun 96	72.1	88	35	20.1	5.49
16 Jul 96	60.6	48	26	10.4	5.57
17 Jul 96	72.3	42	18	6.9	5.92
18 Jul 96	45.1	50	26	9.1	5.22
25 Jul 96	34.9	38	24	5.8	6.15
5 Aug 96	68.5	60	30	16.7	6.39
20 Aug 96	68.9	68	28	18.1	7.18
23 Aug 96	64.4	68	32	17.9	6.04
26 Sep 96	36.4	31	4	-8.3	6.06
2 May 97	78.6	41	17	-0.1	4.12
12 Jun 97	65.5	56	32	13.9	5.21
13 Jun 97	60.1	61	34	16.1	4.54
23 Jun 97	71.0	71	34	20.9	6.37
26 Jun 97	68.3	66	26	14.4	6.98
6 Jul 97	76.1	76	33	18.4	5.31
23 Jul 97	79.1	68	29	16.6	6.38
4 Aug 97	68.4	66	32	16.5	4.81
14 Aug 97	78.0	84	35	23.6	6.95

REFERENCES

Bauman, W. H., III, 1995: Synoptic and mesoscale forcing of convective activity over Cape Canaveral during easterly flow and nowcasting for Space Shuttle landings at Kennedy Space Center. Ph.D. dissertation, North Carolina State University, Raleigh, NC, 140 pp.

Blanchard, D. O., and R. E. Lopez, 1985: Spatial patterns of convection in south Florida. *Mon. Wea. Rev.*, **113**, 1282-1298.

Byers, H. R. and H. R. Rodebush, 1948: Causes of thunderstorms of the Florida peninsula. *J. Meteor.*, **5**, 275-280.

Camp, J. P., A. I. Watson, and H. E. Fuelberg, 1998: The diurnal distribution of lightning over north Florida and its relation to the prevailing low-level flow. *Wea. Forecasting*, **13**, 729-739.

Cummins, K. L., M. J. Murphy, E. A. Bardo, W. L. Hiscox, R. B. Pyle, and A. E. Pifer, 1998: A combined TOA/MDF technology upgrade of the U.S. national lightning detection network. *J. Geophys. Res.*, **103**, 9035-9044.

Donaldson, R. J., R. M. Dyer, and M. J. Krauss, 1975: An objective evaluator of techniques for predicting severe weather events. Preprints: *9th Conf. Severe Local Storms*, Norman, Oklahoma, Amer. Meteor. Soc., 321-326.

Doswell, C. A., III, and J. A. Flueck, 1989: Forecasting and verifying in a field research project: DOPLIGHT '87. *Wea . Forecasting*, **4**, 97-109.

Estoque, M. A., 1962: The sea breeze as a function of the prevailing synoptic situation. *J. Atmos. Sci.*, **19**, 244-250.

Frank, N. L., P. L. Moore, and G. E. Fisher, 1967: Summer shower distribution over the Florida peninsula as deduced from digitized radar data. *J. Appl. Meteor.*, **6**, 309-316.

Fuelberg, H. E. and D. G. Biggar, 1994: The preconvective environment of summer thunderstorms over the Florida panhandle. *Wea. Forecasting*, **9**, 316-326.

Gentry, R. C. and P. L. Moore, 1954: Relation of local and general wind interaction near the sea coast to time and location of air-mass showers. *J. Meteor.*, **11**, 507-511.

Harms, D. E., B. F. Boyd, R. M. Lucci, M. S. Hinson, and M. W. Maier, 1997: Systems used to evaluate the natural and triggered lightning threat to the eastern range and Kennedy Space Center. *Preprint, 28th Conference on Radar Meteorology*, Austin, TX, Amer. Meteor. Soc., 240-241.

Heidke, P., 1926: Berechnung des Erfloges und der Güte der Windstärke-vorhersagen in Sturmwarnungsdienst. *Geogr. Ann. Stockh.*, **8**, 301-349.

Kalnay, E., M. Kanamitsu, R. Kistler, W. Collins, D. Deaven, L. Gandin, M. Iredell, S. Saha, G. White, J. Woollen, Y. Zhu, M. Chelliah, W. Ebisuzaki, W. Higgins, J. Janowiak, K. C. Mo, C. Ropelewski, J. Wnag, A. Leetmaa, R. Reynolds, R. Jenne, D. Joseph, 1996: The NCEP/NCAR 40-year reanalysis project. *Bull. Amer. Meteor. Soc.*, **77**, 437-471.

Kelly, J. L., 1998: Predicting east coast sea breeze initiated convection near Cape Canaveral, Florida. M.S. Thesis, Florida State University, Tallahassee, FL, 49 pp.

Laird, N. F., D. A. R. Kristovich, H. T. Ochs III, R. M. Rauber, and L. J. Miller, 1995: The Cape Canaveral sea and river breezes: Kinematic structure and convective initiation. *Mon. Wea. Rev.*, **123**, 2942-2956.

Lopez, R. E., P. T. Gannon, Sr., D. O. Blanchard, and C. C. Balch, 1984: Synoptic and regional circulation parameters associated with the degree of convective shower activity in south Florida. *Mon. Wea. Rev.*, **112**, 686-703.

Lopez, R. E. and R. L. Holle, 1987: The distribution of summertime lightning as a function of low-level wind flow in Central Florida. *NOAA Technical Memorandum ERL ESG-28.*

Maier, L. M., E. P. Krider, and M. W. Maier, 1984: Average diurnal variation of summer lightning over the Florida peninsula. *Mon. Wea. Rev.*, **112**, 1134-1140.

Mielke, P. W., K. J. Berry, and E. S. Johnson, 1976: Multi-response permutation preocedures for a priori classifications. *Commun. Statist. Theor. Meth.*, **A5**, 1409-1424.

Mielke, P. W., K. J. Berry, and G. W. Brier, 1981: Applications of multi-response permutation procedures for examining seasonal changes in monthly sea-level pressure patterns. *Mon. Wea. Rev.*, **109**, 120-126.

Neumann, C. J., 1971a: Thunderstorm forecasting at Cape Kennedy, Florida, utilizing multiple regression techniques. *NOAA Technical Memorandum NWS SOS-8.*

Neumann, C. J. 1971b: The thunderstorm forecasting system at the Kennedy Space Center. *J. Appl. Meteor.*, 10, 921-936.

Orville, R. E., Jr., 1987: An analytical solution to obtain the optimum source location using multiple direction finders on a spherical surface. *J. Geophys. Res.*, **92**, 10 877 – 10 886.

Orville, R. E., Jr., 1991: Annual Summary Lightning ground flash density in the contiguous United States – 1989. *Mon. Wea. Rev.*, **119**, 573-577.

Orville, R. E., Jr., 1994: Cloud-to-ground lightning flash characteristics in the contiguous United States. *J. Geophys. Res.*, **99**, 10 833-10 841.

Panofsky, H. A., and G. W. Brier, 1958: *Some Applications of Statistics to Meteorology*, Pennsylvania State University Press, p. 200 ff.

Pielke, R. A., 1974: A three-dimensional numerical model of the sea breezes over South Florida. *Mon. Wea. Rev.*, **102**, 115-139.

Reap, R. M., 1994: Analysis and prediction of lightning strike distribution associated with synoptic map types over Florida. *Mon. Wea. Rev.*, **122**, 1698-1715.

Watson, A. I. , R. E. Lopez, R. L. Holle and J. R. Daughtery, 1987: The relationship of lightning to surface convergence at Kennedy Space Center: A Preliminary study. *Wea Forecasting*, **2**, 140-157.

Watson, A. I., R. L. Holle, R. E. Lopez, R. Ortiz, and J. R. Nicholson, 1991: Surface wind convergence as a short-term predictor of cloud-to-ground lightning at Kennedy Space Center. *Wea. Forecasting*, **6**, 49-64.

Watson, A. I. and R. L. Holle, 1996: An eight year lightning climatology of the southeast United States prepared for the 1996 Summer Olympics. *Bull. Amer. Meteor. Soc.*, **77**, 883-890.

Wilks, D. S., 1995: *Statistical Methods in the Atmospheric Sciences*, Academic Press, 464 pp.